universität wien

MASTERARBEIT / MASTER'S THESIS

Titel der Masterarbeit / Title of the Master's Thesis

Secondary metabolite production during sexual development in *Trichoderma reesei* and its analysis by HPTLC and DESI-MS

verfasst von / submitted by

Ezgi Özkan

angestrebter akademischer Grad / in partial fulfilment of the requirements for the degree of

Master of Science (MSc)

Wien, 2020/ Vienna, 2020

Studienkennzahl lt. Studienblatt / degree programme code as it appears on the student record sheet:	UA 066 877
Studienrichtung lt. Studienblatt / degree programme as it appears on the student record sheet:	Masterstudium Genetik und Entwicklungsbiologie
Betreut von / Supervisor:	PD Dr. Monika Schmoll

Acknowledgements

I would Like to thank my supervisor PD Dipl. -Ing. Dr Monika Schmoll PhD for giving me this opportunity to work on this exciting project for my master thesis, and I would like to thank her not only for her support and guidance throughout my work but also for reading my thesis critically.

Special thanks to Dipl. -Ing. Dr Stefan Böhmdorfer for introducing me to the work in an analytical chemistry laboratory and guiding me through each detail with patience. I also want to thank him and Univ. Prof. Dipl. -Chem Dr.rer.nat. Dr.h.c. Thomas Rosenau for expanding my vision by letting me work creatively within their technical team.

I would also like to thank Wolfgang Hinterdobler, for being a great tutor and assisting me through my entire master thesis, also helping me to plan my setup, which was a key point to deal with a two-parted assignment.

Many thanks to my colleagues from AIT, Irene, Dania, Samira, Sabrina; and my colleagues from BOKU.

I am grateful for funding for my thesis from FEMtech.

Further on, I would like to express my deepest thanks to my parents and my dear sister Özge for their love and never-ending remote support.

Also Ginger and Paco for reminding me to take a break by sitting on my laptop.

Finally, I am extremely thankful to Johannes for being always on my side, no matter what supporting me and never hesitating to show me his love.

Abstract

The heterotrimeric G-protein signalling pathway is one of the most crucial signal transduction pathways for filamentous fungi including *Trichoderma reesei*. One of the essential functions of this pathway in *T. reesei* is sensing the potential mating partners in the vicinity.

In this study we aimed to investigate how G-protein mediated signalling affects partner sensing, recognition and establishment of an adequate communication between potential mating partners. Therefore, we have screened the effects of each one of the G-protein subunits; alpha, beta and gamma, as well as the effects of G-protein coupled pheromone receptors and precursor, in terms of partner sensing and chemical communication during the sexual development using High Performance Thin Layer Chromatography (HPTLC).

Consequently, we were able to show the impact of the G-protein coupled pheromone signalling machinery during sexual development not only by receiving and transmitting the pheromone signals but also by being part of the fine-tuning mechanism for the secretion of the secondary metabolites in case of encountering another fungus.

HPTLC is a widely used technique for investigating secondary metabolites. However, it is currently problematic to determine the identity of the separated bands throughout the HPTLC plates without tedious extraction and sample preparation. For this reason, there have been various attempts to couple HPTLC with Desorption Electrospray Ionization – Mass Spectrometry (DESI-MS), which is a reliable tool for identifying the substances.

Moreover we have successfully developed a feasible method for coupling HPTLC with DESI-MS. This method allows to rapidly identify certain substances, that are separated and screened on HPTLC by assigning them to mass spectrometry analysis without disrupting the derivatization steps following in HPTLC analysis. Additionally, this coupling method is a candidate for secondary metabolite profiling.

Abstrakt

Der heterotrimerische G-Protein Signalpfad ist eine der wichtigsten Signal-Transduktionspfade filamentöser Fungi, wie zum Beispiel *Trichoderma ressei*. Eine der essenziellen Funktionen dieses Pfades in *T. reesei* ist es, in ihrer Umgebung potenzielle Partner für ihre Fortpflanzung wahrzunehmen.

In dieser Studie haben wir untersucht, wie G-Protein vermittelte Signalisierung die Wahrnehmung, die Erkennung und die Herstellung einer Kommunikation mit einem potenziellen Sexualpartner beeinflusst. Deswegen haben wir die Effekte aller G-Protein Untergruppen überprüft; Alpha, Beta und Gamma sowie die Effekte der mit G-Protein verkoppelten Pheromon-Rezeptoren und Pheromon-Vorläufer, bezüglich der Wahrnehmung von Sexualpartnern und der chemischen Kommunikation während der sexuellen Entwicklung unter Verwendung von Hochleistungs-Dünnschichtchromatographie (HPTLC).

Folglich waren wir in der Lage zu zeigen, dass die mit G-Protein-gekoppelte Pheromon-Signalisierungs-Maschinerie Einfluss während der sexuellen Entwicklung ausübt, nicht nur durch Erhalten, sondern und durch Senden der Pheromon-Signale, sondern auch dadurch, dass sie Teil des Feinabstimmungs-Mechanismus ist.

HPTLC ist ein weitverbreitetes Verfahren, um sekundäre Metaboliten zu untersuchen. Allerdings ist es derzeit problematisch die Identität der getrennten Bänder ohne langwierige Extraktion und Probenvorbereitung durch die HTPLC Platten zu bestimmen. Das ist der Grund warum es zahlreiche Versuche gegeben hat, um HTPLC mit Desorption Elektrospray-Ionisation zu verbinden Massenspektronomie (DESI-MS), welches ein verlässliches Werkzeug zur Identifikation von Substanzen ist.

Darüber hinaus haben wir erfolgreich eine Methode entwickelt, um HPTLC mit DESI-MS zu verbinden. Diese Methode erlaubt es bestimmte Substanzen rasch zu identifizieren, welche auf HPTLC aufgeteilt und untersucht wurden, indem man sie zur Massenspektronomie-Analyse überträgt, ohne die Schritte der Derivatisierung in der HTPLC-Analyse zu unterbrechen. Zusätzlich ist diese Methode ein Kandidat für das sekundäre Metaboliten-Profiling.

Table of Contents

1. Introduction

1.1. *Trichoderma* in the Kingdom of Fungi

Filamentous fungi can rapidly form extensive mycelial networks. This quick growth gives them the advantage to seek, adhere and invade new ecological niches rather quickly. Therefore, they are evolutionarily very successful (Busch & Braus, 2007). Filamentous mesophilic ascomycete *Trichoderma* spp. is a soilborne genus that is found in the root and its surroundings (Harman *et al.*, 2004).

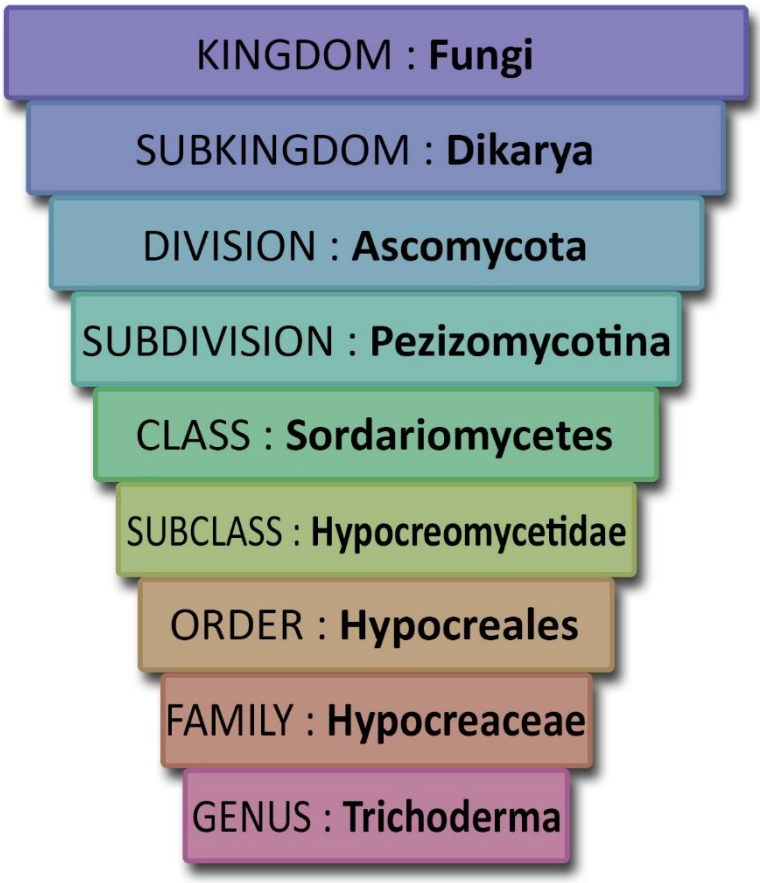

Figure 1. *Classification of the species Trichoderma reesei (information retrieved from Simmons E. G., 1977).*

Trichoderma spp. are considered to be successful colonizers when they are introduced to new environments. This is the result of rapid adaptation of the species to the surroundings by adjusting their quick response to light and to utilizing existing resources like decaying plants. Therefore, they can be found in various ecosystems (Kubicek *et al*. 2008).

Due to their characteristic features, such as their defence mechanisms or their capability to quickly expand into new environments, *Trichoderma* spp. are one of the most studied genera of fungi (Schuster & Schmoll, 2010). These various abilities of the genus attracted a lot of attention in several areas like in agriculture due to its crucially important beneficial impacts on plant growth and fighting against various plant pathogens in natural and synthetic ecosystems (Harman *et al.*, 2004).

1.2. *Trichoderma reesei*: Ingenious member of the *Hypocreaceae* Family

Trichoderma reesei, the anamorph of *Hypocrea jecorina*, is one of several hundred species of the genus *Trichoderma/Hypocrea*, the classification of which is shown in figure 1. *T. reesei/H. jecorina* was the first sequenced member of the genus (Druzhinina *et.al.*, 2006).

The discovery of *Trichoderma reesei* goes back to the early 20th century. *T. reesei* was at first isolated because of its damaging effect on US Army equipment on the Solomon Islands during World War II. Nevertheless, with the discovery of the impressive cellulose degradation ability, researchers turned *T. reesei* into an industrial workhorse (Bischof *et al.*, 2016). Therefore, the potent degrader *T. reesei* has been used in various fields due to its ability to degrade cellulose with cellulase and the production of cellulase can be used in divergent purposes such as an alternative to chlorine bleaching or as an alternative to washing powder (Samuels, 1996). The reference strain of *T. reesei* "QM6a" is the last remaining original wild type strain, from which most of the industrially used strains, as well as most of the laboratory strains, are derived (Bischof *et al.*, 2016).

1.2.1. Sexual development in *T. reesei*

Sexual development has evolved to increase competitiveness. Consequently, it's based on extending variety by generating a diversity through recombination of the genes. Therefore, it's superior to asexual development, in terms of survival against changing environmental conditions (Heitman *et. al.*, 2013). Sexual development, in general, requires the sensing of a potential mating partner and the ability to recognize mating partners can be affected by various environmental factors, however, light has a special impact on the decision whether asexual or sexual development is to be preferred (Seidl *et al.*, 2009; Schmoll, 2013).

Trichoderma was for a long time considered anamorph, meaning it is only reproducing asexually, since mimicking the natural mating conditions of a fungus under controlled laboratory conditions is complicated (Schmoll, 2013). But in the last decade, studies showed otherwise (Seidl *et al.*, 2009), and it was proved that the lack of sexuality does not automatically mean asexuality. Considering the sexual mating conditions differ strongly depending on environmental conditions and contain multiple criteria such as light, nutritional conditions, humidity and sexual development is regulated by a complex fine-tuning machinery (Schmoll, 2013).

1.2.2. Sexual mating types in *T. reesei*

In the fungi kingdom mating takes place heterothallic, among two different mating types, or homothallic, in which the fungus mates with itself (Heitman *et al.*, 2013). Although the determination of sex by mating type is not clear yet, the female character is assumed to be the one which makes the investment of resources to form fruiting bodies (Heitman *et al.*, 2013).

Successful heterothallic sexual reproduction in fungi is the result of crossing two suitable mating partners. The definition of the mating types MAT1-1 and MAT1-2 in the filamentous ascomycete comes from the difference in the sequences of the specific MAT loci, which is occupying the same genomic locus where the transcriptional regulators are encoded (Schmoll, 2013; Seidl *et al.*, 2009).

T. reesei QM6a, which has the mating type MAT1-2, is considered to be a female sterile strain due to its inability to form fruiting bodies with the opposite mating type. When it's crossed with other strains, it can act as a male partner (Seidl *et al.*, 2009).

1.2.3. Fruiting bodies and ascospores

Growth by asexual hyphal structures is generally adequate in terms of survival under no stress conditions. However, some fungi can advance this growth converting their filamentous structure into multicellular, unitary, container-like perithecia, which protect the meiotically derived spores with a densely packed outer envelope (Busch & Braus, 2007).

Filamentous fungi have to reach a certain competence state, which is the growth rate of the specific fungus, as vegetative hyphae, to be able to respond to environmental signals like nutrients, light, pheromones, to differentiate into sexual unitary fruiting bodies (Bayram & Braus, 2012). The transition from the vegetative growth to the development of the fruiting bodies requires more energy, therefore the resulting alteration does not occur because of cell necessities but as a result of environmental factors or endogenous autoregulatory signals (Busch & Braus, 2007).

Members of the kingdom fungi disperse their spores through air and water to colonize new environments. Sexual spores, called ascospores, are produced in asci, which are specific cell types to bare spores. Asci are located inside of perithecia, which are small tubular sacs, and discharge their ascospores into the air with the pressure force inside of the ascus, as if they were fungal canons (Trail, 2007). Additionally, the fruiting body structure serves as a shelter and protects the ascospores from harsh conditions (Bayram & Braus, 2012).

1.3. Secondary metabolism

Filamentous fungi can synthesize various secondary metabolites (Bayram & Braus, 2012), which are involved in survival mechanisms against fungivorous preys and predators for competition and defence, and they are not directly involved in regular metabolic events (Zeilinger *et al.* 2016). Because of this ingenuity, *Trichoderma* species are used quite commonly as commercial bio-fungicides in the industry of agriculture and *Trichoderma* derived secondary metabolites have a large potential to be drug compounds (Zeilinger *et al.* 2016). Furthermore, some of the secondary metabolites serve as a molecule to generate a language to maintain interspecies communication through their signalling pathways (Speckbacher & Zeilinger, 2018).

Trichoderma species can produce low-molecular-weighted volatile secondary metabolites that have long-distance effects as well as high-molecular-weighted non-volatile secondary metabolites that have a relatively shorter range (Cardoza *et al.*, 2005). Genes that are involved in the biosynthesis of the secondary metabolism in *Trichoderma* species are not yet fully understood, due to the fact that *Trichoderma* is capable of producing large numbers of secondary metabolites simultaneously (Cardoza *et al.*, 2005).

Trichoderma derived secondary metabolite biosynthesis involves various genetic mechanisms and large numbers of regulations on cellular processes in their biochemical pathways, these allow species-specific secondary metabolite secretion and species-specific phenotype formation for different species of the genus (Zeilinger *et al.* 2016).

It was discovered that *Trichoderma* genomes harbour multiple secondary metabolism-related gene clusters, which contain specific transcription factors. The expression patterns of these genes located in the clusters are influenced by the presence of numerous external biotic and abiotic factors; namely, light, nutrients and other microorganisms. Consequently, the secondary metabolite machinery is activated by GPCRs, by sensing the individual environmental cues that are transmitted through G-

protein signalling pathway and followed by multiple downstream intracellular signalling pathways (Zeilinger *et al.* 2016).

In *Trichoderma reesei* secondary metabolites are not known to be harmful compounds, these metabolites, together with the pheromone systems, are involved in sensing the potential mating partner in the vicinity and in the chemical communication with the mating partners, furthermore, secondary metabolites are involved in sexual development (Bazafkan *et al.*, 2015; Dattenböck *et al.*, 2018).

1.4. Signal transduction pathways in *Trichoderma reesei*

Mechanisms that are involved in the regulation of sexual development of *T. reesei* are under investigation ever since its sexual development was discovered. Signal transduction pathways are sequences of molecular events followed by cellular responses and they are essential for regulating the sexual development in *T. reesei* in terms of transmitting important information (Schmoll, 2013).

1.4.1. G-protein coupled receptors and signalling pathways

In terms of survival, a cell needs to sense and respond to the extracellular signals. The heterotrimeric G-protein system is one of the most important members of the extracellular signalling pathways (Schmoll 2013). The highly conserved G- protein signalling pathway consists of heterotrimeric G-protein and a G-protein coupled receptor (GPCR), a seven-fold transmembrane receptor associated with the heterotrimeric G-protein (Yu, 2006).

The extracellular receptor GPCR is located on the plasma membrane and it connects the cell to the environment with its extracellular N-terminus that senses the external signal, which then gets transmitted to the intracellular C-terminus (Gruber *et al.*, 2013). A canonical heterotrimeric G-protein, which is composed of α, β and γ subunits, is coupled to the C-terminus of the GPCR with its α subunit (Li *et al.*, 2007).

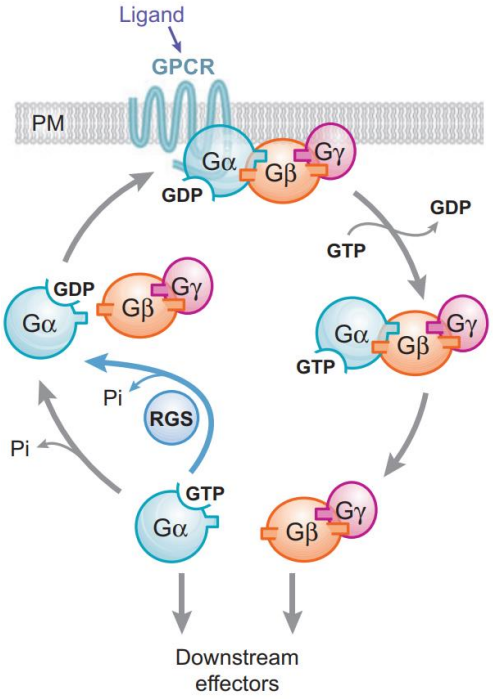

Figure 2. *G-protein coupled receptor (GPCR) mediated signalling. An external signal gets transferred to the cytoplasm via the GPCR. Ligand binding activates the inactive G-protein complex, causing the disassociation of the β and γ subunits from the α subunit. Gα-GTP and Gβγ are free to regulate downstream pathways (retrieved from Li et al., 2007).*

In the absence of a ligand, an inactive heterotrimeric G-protein complex is bound to the GPCR and all three subunits reside in the complex alongside a GDP that is bound to the α subunit. Ligand binding to the extracellular N-terminus of the GPCR activates the receptor and this activation causes the exchange of GDP with GTP, which leads to the dissociation of β and γ subunits from the complex as a dimer simultaneously. This dissociation sets both Gα-GTP and Gβγ subunits free to bind to several downstream factors to regulate their activities resulting in the propagation of the initial signal (Figure 2) (Li *et al.*, 2007; Gruber *et al.*, 2013; Schmoll, 2013; Yu, 2006).

GTPase activity of G-protein α subunits leads to the GTP hydrolysis and GDP bound Gα is ready to bind to a Gβγ dimer. This reassociation leads to the inactive state of the complex, which is once again able to reinitiate the cascade. Thence Gα subunits are the signal switches of the cascade while controlling the duration and the intensity of the signal transduction with the rate of the hydrolysation action (Yu, 2006; Li *et al.*, 2007).

The heterotrimeric G-protein signalling pathway of *Trichoderma reesei*, as in many other filamentous fungi, has three α subunits of G-protein, GNA1, GNA2 and GNA3, one Gß subunit and one Gγ subunit (Schmoll, 2008).

GNA1 is involved in the restriction of intracellular cAMP levels by inhibiting adenyl cyclase. This inhibition leads to the inability of converting the ATP into cyclic AMP. Additionally, GNA1 is involved in the regulation of the cellulase gene transcription (Seibel *et al.*, 2009). Furthermore, they play a role in stress and growth regulation, depending on the carbon source and light status, resulting to be an important factor in the whole signalling cascade. Additionally, they are linked to the mammalian $G\alpha_i$ superfamily proteins (Seibel *et al.*, 2009).

The function of the GNA2 is not yet well identified and they are not as well conserved as the other α subunits (Li *et al.*, 2007). In contrast to the GNA1, GNA3 is involved in increasing intracellular cAMP levels indirectly by activating adenyl cyclase, which gives it the homology to mammalian $G\alpha_s$ proteins. Moreover, GNA3 is involved in the positive regulation of cellulase gene expression with the presence of light (Schmoll *et al.*, 2009; Seibel *et al.*, 2009).

Seibel *et al.* suggest that in *T.reesei*, each GNA transmits multiple signals due to the fact that it has 58 predicted G-Protein coupled receptors (Gruber *et al.*, 2013) but only three Gα subunits (Seibel *et al.*, 2009; Schmoll, 2008).

G-protein ß and γ subunits are well conserved within the filamentous fungi. G-protein ß and γ subunits are essential for acquiring the stability of each other for the heterodimer formation (Li *et al.*, 2007). Class I phosducin like proteins (PhLP1) are assumed to be the junction protein for Gßγ heterodimer assembly and PhLP1 enhances the function of the dimer while acting as a molecular chaperone (Schmoll, 2013). PhLPs are positive regulators of Gßγ heterodimers on their downstream signalling levels and PhLPs are required for controlling the standard levels of Gß and Gγ subunits (Yu, 2006).

In *Trichoderma reesei*, G-protein signalling pathways play essential roles in fine-tuning mechanisms of various biological functions such as sexual development (Schmoll, 2013), cellulase gene expression (Schmoll *et al.*, 2010), nutrient signalling and light response (Gruber *et al.*, 2013).

1.4.1.1. Pheromone modulated signalling through G-protein signalling pathways

The pheromone system is one of the critical communicational cascades of *T. reesei* during sexual development. This cascade is utilized for communication between the potential mating partners in proximity for a successful mating through their G-protein coupled pheromone receptors HPR1, HPR2 and compatible peptide pheromone precursors HPP1, PPG1 transmitting the signal which is then received by the HPR1 and HPR2 respectively (Bazafkan *et al.,* 2015; Schmoll, 2013). This whole complex machinery is very crucial to *T. reesei* for partner sensing and sexual development, therefore

it ensures the functioning of the machinery, it is highly regulated by numerous factors (Bazafkan *et al.*, 2017).

Pheromone receptors are essential for female fertility, lack of the receptor in their cognate mating type results in female sterility. Besides this, availability of the pheromone precursors is essential for male fertility (Seibel *et al.*, 2012).

2. Materials and Methods

2.1. Strains and culture conditions

Several *T. reesei* wild type strains from different sources and several derivatives of these wild type strains were analysed under asexual and sexual growth conditions. They were crossed with the fully fertile wild type strain CBS999.97 MAT1-1 (Seidl *et al.*, 2009). Thereby we were able to create a confrontation zone of two compatible mating partners. With this set-up, we studied the secondary metabolite production and chemical communication under controlled conditions (Table 1).

Table 1. *List of the strains used in this study.*

Strain	Back-ground	Characteristics	Reference
TU-6	WT	Uridine auxotrophic wild type strain	Gruber *et al.* (1990)
QM9414	WT	Female sterile wild type strain	Schuster *et al.* (2012)
QM6a	WT	Original female sterile wild type isolate	Martinez *et al.* (2008)
CBS1-1	WT	Fully fertile wild type strain CBS999.97	Seidl *et al.* (2009)
Δgna1	TU-6	G-protein α1 subunit deletion mutation	Seibel *et al.* (2009)
Δgna2	TU-6	G-protein α2 subunit deletion mutation	Schuster *et al.* (2012)
Δgna3	TU-6	G-protein α3 subunit deletion mutation	Schuster *et al.* (2012)
gna1QL	TU-6	Constitutively activated G-protein α1 subunit	Seibel *et al.* (2009)
gna2QL	QM6a	Constitutively activated G-protein α2 subunit	Rodriguez Iglesias (unpublished)
gna3QL	TU-6	Constitutively activated G-protein α3 subunit	Schmoll *et al.* (2009)
Δgnb1	QM9414	G-protein β subunit deletion mutation	Tisch *et al.* (2011b)
Δgng1	QM9414	G-protein γ subunit deletion mutation	Tisch *et al.* (2011b)
Δphlp1	QM9414	Class I phosducin-like protein deletion mutation	Tisch *et al.* (2011b)
Δhpr1	QM6a	Pheromone receptor deletion - compatible pheromone precursor HPP1	Seibel *et al.* (2012)
Δhpr2	QM6a	Pheromone receptor deletion - compatible pheromone precursor PPG1	Seibel *et al.* (2012)
Δhpp1	QM6a	Pheromone precursor deletion - compatible pheromone receptor HPR1	Schmoll *et al.* (2010)

Before the inoculation, strains were revived from -80°C storage, thereafter each strain was propagated on 3% (w/v) malt extract agar (Merck, Darmstadt, Germany) at 28°C. Fully grown petri dishes were used for inoculation on 2% (w/v) malt extract agar with 2 cm^2 (0.5 cm x 4 cm) agar slices. Agar plugs were placed near the margin (as shown in Figure 4). This setup guarantees an even confrontation line for harvest (Hinterdobler *et al.*, 2019). Ultimately, each strain was used in 9 sexual cultivations for studying the confrontation and the fruiting body formation and in 9 asexual cultivations. Furthermore, for the phenotype analysis, there were 2 additional cultivations, which were prepared using ~0.2 cm^2 ($(0.5\ cm)^2 \times \pi$) agar slices from each strain exclusively.

T. reesei strain TU-6 is a derivative of QM9414, which is incapable of synthesizing uridine that is required for the fungus' growth (Gruber *et al.*, 1990). Thus, for the auxotrophic TU-6 strain, both the propagation agar and the inoculation malt extract agar were prepared with the addition of 10 mM uridine.

Eventually, the samples were incubated at 22°C for 14 days at 1700 lux under the 12 hours light 12 hours of dark conditions.

After 14 days of incubation, each sample was visually analysed for the phenotypic differences and photographed.

2.2. HPTLC sample preparation

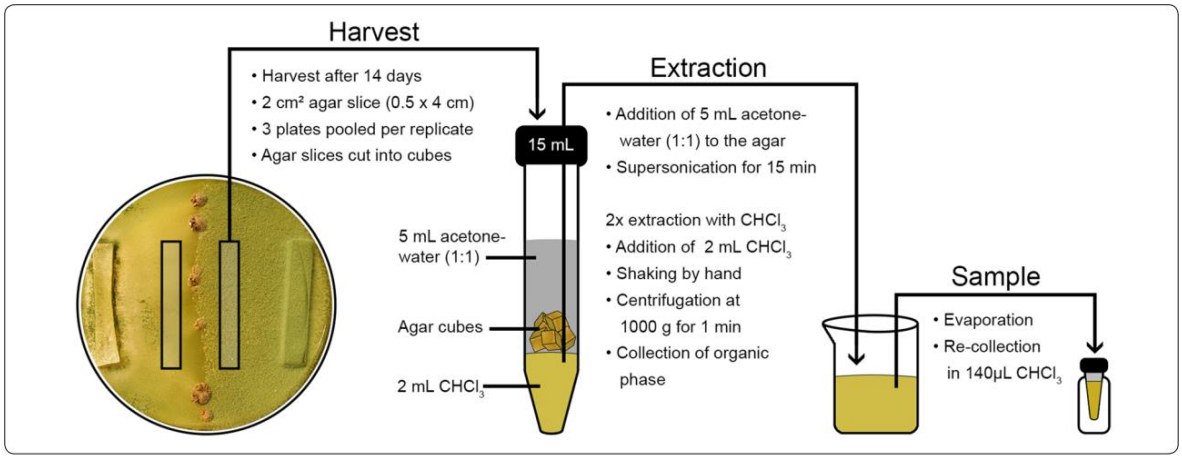

Figure 3. *Sample preparation for the HPTLC. After incubation of the samples, agar slices were pooled in three biological replicates. Thereafter, the extraction of the samples was done accordingly, to analyse with the HPTLC (Retrieved from Hinterdobler et al., 2019).*

Extraction of secondary metabolites from two weeks old cultures was done according to a published protocol (Bazafkan *et al.*, 2015) with small alterations. Agar slices, in the proximity of the confrontation zone in the sexual petri dishes and for precise assaying equivalent zone from the asexual petri dishes, were obtained in the size of 2 cm^2 as it was done for inoculation. Agar pieces from three petri dishes were pooled in one independent biological replicate in account of having three biological replicates from each strain under sexual and asexual conditions.

Each one of the three biological replicates was placed in 15 ml centrifugation tubes and secondary metabolites were extracted by 15 minutes of sonication of the mixture of agar slices with 5 ml 50% acetone in water. Immediately after the sonication, 2 ml of chloroform ($CHCl_3$) was added and centrifuged at 4°C with 1000 g for one minute. To obtain the organic phase as completely as possible, chloroform separation was performed twice. The organic phase was then transferred to the glass vials for overnight evaporation. Consequently, after the complete evaporation of the solvent, dry extracts were resuspended in 140 µl chloroform and placed in HPTLC vials (Figure 3).

2.3. HPTLC analysis

2.3.1. Sample application

For the HPTLC analysis of secondary metabolites, samples were arranged in such a way so that the related samples would be aligned with each other and the conclusive visual assaying would be viable. With the consideration of this adjustment, 5 µl of the secondary metabolite samples were sprayed onto glass-backed high-performance thin-layer chromatography silica gel plates with a fluorescent indicator (HPTLC plate, silica gel 60, 200 x 100 mm, E. Merck, Darmstadt, Germany), by an automatic TLC sampler (ATS 4, CAMAG, Muttenz, Switzerland). Each silica gel plate bore 30 selected samples with 4.5 mm band length and 5.5 mm track distance. The amount of 5 µl was chosen to attain clear patterns and yet not to overload the plate (Bazafkan *et al.*, 2015).

2.3.2. Developing HPTLC plates

The following step after sample application was developing the samples in an Automated Development Chamber (ADC 2, CAMAG, Muttenz, Switzerland) with the help of the eluent. The

separation was performed using 7:1 (v/v) ratio of water extracted $CHCl_3$ and 1 mM TFA (Trifluoroacetic Acid) in methanol as mobile phase at 11% humidity and solvent front flow distance of 70 mm.

2.3.3. Scanning and visualizing

Developed samples were analysed for the secondary metabolite patterns. In the first place, an investigation was done visually while capturing the images of the HPTLC plates at different illumination modes, white light (daylight), UV 254 nm and UV 366 nm with a visualizer (TLC Visualizer, CAMAG, Muttenz, Switzerland). Thereafter the samples went through a quantitative densitometric analysis which covered seven different wavelengths (254 nm, 290 nm, 345 nm, 366 nm, 420 nm, 470 nm and 520 nm) using a TLC Scanner (TLC Scanner 3, CAMAG, Muttenz, Switzerland).

Anisaldehyde Sulfuric Acid (AS) is a reagent for detection of the potential bioactive compounds because of its sensitivity to many functional groups upon mild heating (Gerlach *et al.*, 2018). Derivatization with *p*-anisaldehyde : sulfuric acid reagent reveals specific colours for different compounds thus allows the detection of them in non-quantitative fashion.

HPTLC plates were derivatized in *p*-anisaldehyde : sulfuric acid reagent and heated up to 120° to be able to get the maximum visualisation possible. Lastly, the HPTLC plates were visualized once again at same illumination modes as before derivatization: white light, UV 254 nm and UV 366 nm with a visualizer (TLC Visualizer, CAMAG, Muttenz, Switzerland).

All the densitometric evaluation and image documentation data was recorded and analysed with an HPTLC software called visionCATS (VisionCATS 2.5, CAMAG, Muttenz, Switzerland).

3. Results

In this study, we aimed to analyse the G-protein and receptor-mediated alteration of the secondary metabolite pattern of the *Trichoderma reesei* during sexual development in detail. Therefore, initially, we compared phenotype pictures of the cognate mutations according to the conidiation rings and the fruiting bodies. Thereafter, we applied HPTLC to detect different secondary metabolite production pattern of the mutations.

3.1. G-protein α subunits

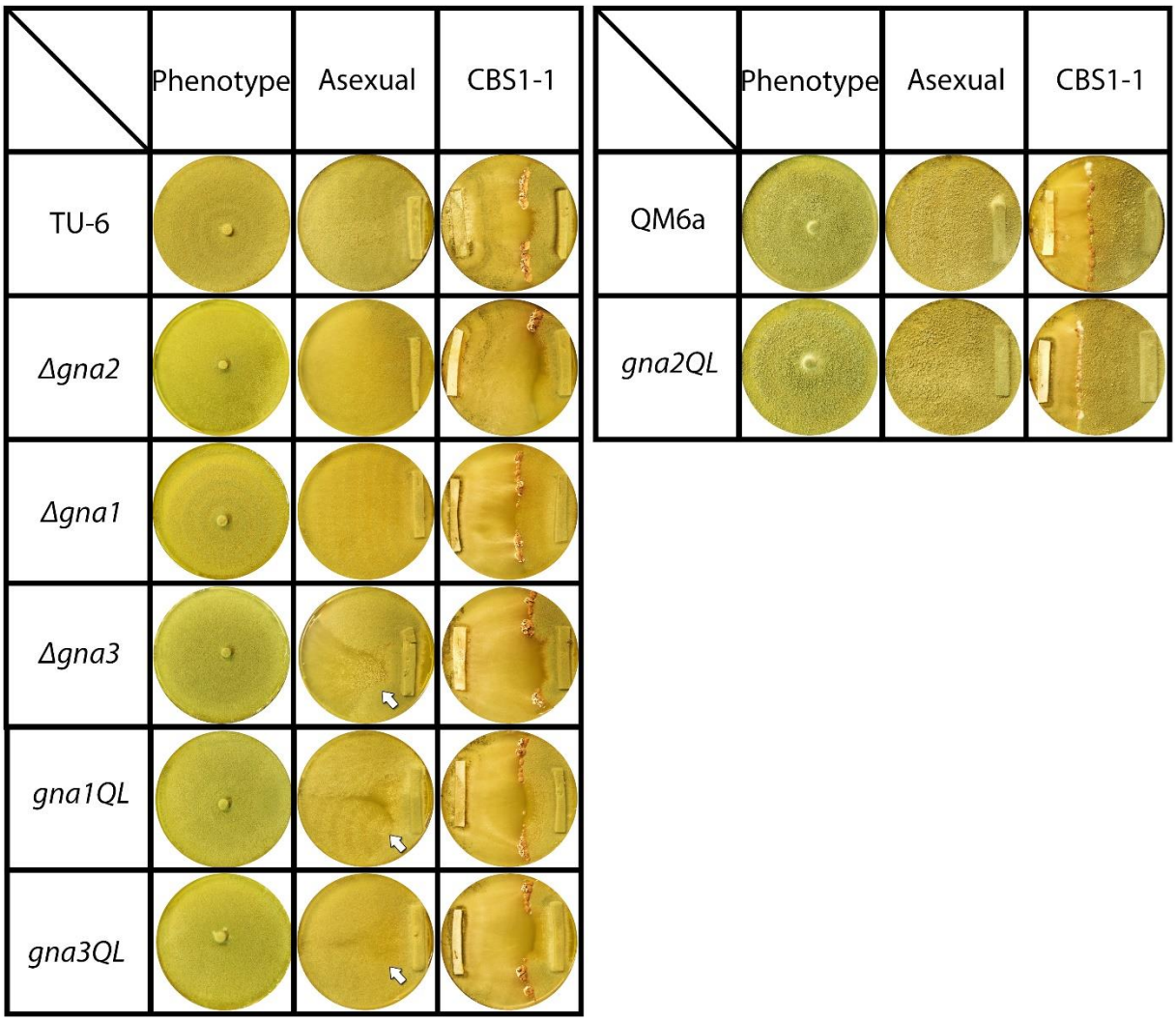

Figure 4. *Phenotype pictures of G-protein α subunit deletions and over expressions after 2 weeks of inoculation under 22°C, 1700 lux, 12 hours light - 12 hours dark conditions. Deletion mutations are shown on the left side. All the deletion mutations of G-protein α subunits have TU-6 background (shown on the left side). Constitutive activations of the G-protein α subunits GNA1 and the GNA3 are from the TU-6 background (shown on the left side). Constitutive activations of the G-protein α subunits the GNA2 are from the QM6a background (shown on the right side). Strains were grown on 2% (w/v) malt extract agar.*

3.1.1. G-protein α subunits don't have a major impact on sexual development

Phenotype observations show that each strain had successful mating with the fully fertile wild type strain CBS999.97 (Figure 4). Fruiting body formations of each crossing reveal that neither the deletion nor the constitutive activation of the G-protein α subunits were inhibiting factors for the sexual development.

These results were similar to the previously published studies for GNA1 (Seibel *et al.*, 2009), GNA2 (Schuster *et al.*, 2012) and GNA3 (Schmoll *et al.*, 2009; Schuster *et al.*, 2012).

3.1.2. G-protein α subunits moderately influence the conidiation ring formation

After two weeks of incubation under controlled light conditions (12 hours light - 12 hours dark) mutant strain *Δgna3* and the constitutive activations of GNA1 and GNA3 exhibited slightly decreased conidiation ring formations (Figure 4, Highlighted with arrows). Conidiation was not influenced by the deletion of GNA1 and the over expressions of GNA1 and GNA2 (Figure 4).

3.1.3. Secondary metabolite production is affected by G-protein α subunits

We were interested whether GNAs were involved in the production of the secreted metabolites, therefore, we analysed G-protein α subunit mutations with the mutants that grew alone and in the presence of a mating partner alongside with the wild type combinations as controls.

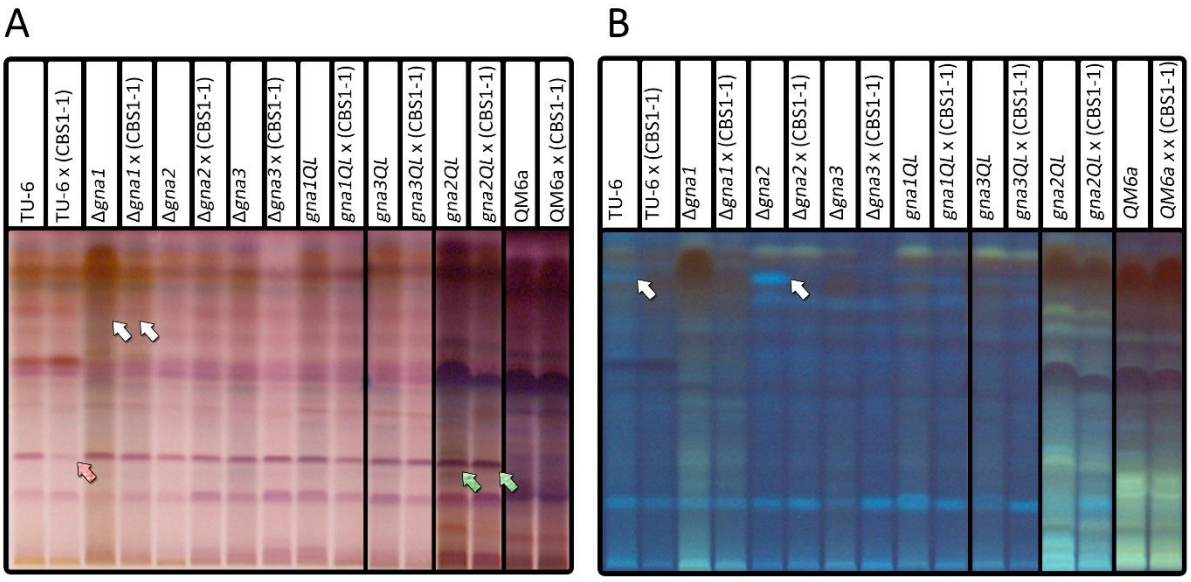

Figure 5. *Secondary metabolite production patterns of T. reesei G-protein α mutant strains under asexual and sexual conditions. See table 1 for sample codes. Different visualisation techniques were applied to detect different substances at each panel and to enable optimal comparison between samples, pictures were reassembled. The corresponding wild type of gna2QL is QM6a; TU-6 is the corresponding wild type of the rest.* ***A.*** *Derivatized with anisaldehyde – sulfuric acid, visible light.* ***B.*** *UV light at 366 nm. Analyses were done in three biological replicates. Replicates were consistent. See supplementary figure 1a-f for other replicates.*

Deletion mutation of the GNA1 exhibits a clear difference in the sorbilicilin derivative secondary metabolite pattern when it grew alone (Figure 5a, highlighted with a white arrow (left)), however, when there is a mating partner in the vicinity the metabolite pattern resembles the other G-protein α subunit mutations that grew in the presence of a mating partner (Figure 5a, highlighted with a white arrow (right)).

In the wild type conditions, the presence of a mating partner causes a specific response for the secretion of the highlighted compound, production of which gets increased upon deletion and constitutive activation of the G-protein α subunits (Figure 5a, Highlighted with a red arrow).

Upon constitutive activation of GNA2, the highlighted compound gets significantly upregulated (Figure 5a, Highlighted with green arrows).

The wild type strain produces a compound with blue fluorescence, which is not produced when there is a potential mating partner in the vicinity and this component gets clearly upregulated when the strain has *Δgna2* mutation (Figure 5b, Highlighted with white arrows).

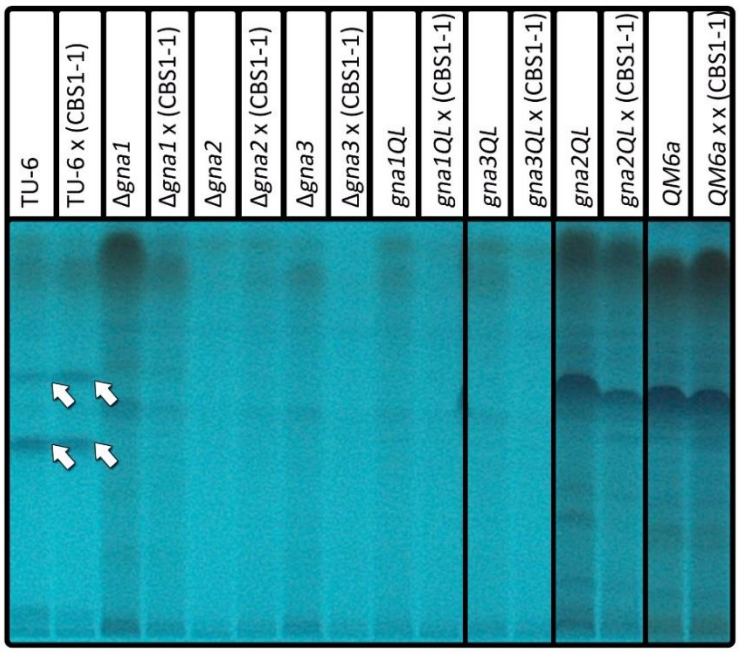

Figure 6. *Secondary metabolite production patterns of T. reesei G-protein α mutant strains under asexual and sexual conditions. See table 1 for sample codes. Different visualisation techniques were applied to detect different substances at each panel and to enable optimal comparison between samples, pictures were reassembled. The corresponding wild type of gna2QL is QM6a; TU-6 is the corresponding wild type of the rest. UV light at 254 nm. Analyses were done in three biological replicates. Replicates were consistent. See supplementary figure 1g-i for other replicates.*

Upon deletion as well as the overexpression of the G-protein α subunits, at least two of the secreted compounds get clearly reduced with the mutants that grew alone as well as with the mutants that encountered a potential mating partner (Figure 6, Highlighted with white arrows). We observed the scanning densitometry of the HPTLC chromatogram for additional UV-VIS information of the statement above. HPTLC fingerprint profile of TU-6 showed elevated levels of peaks around R_f 0.4 and at R_f 0.5 at all three replicates, which is contradictory to the mutation scanning at the related wavelength of 254 nm (Figure 7).

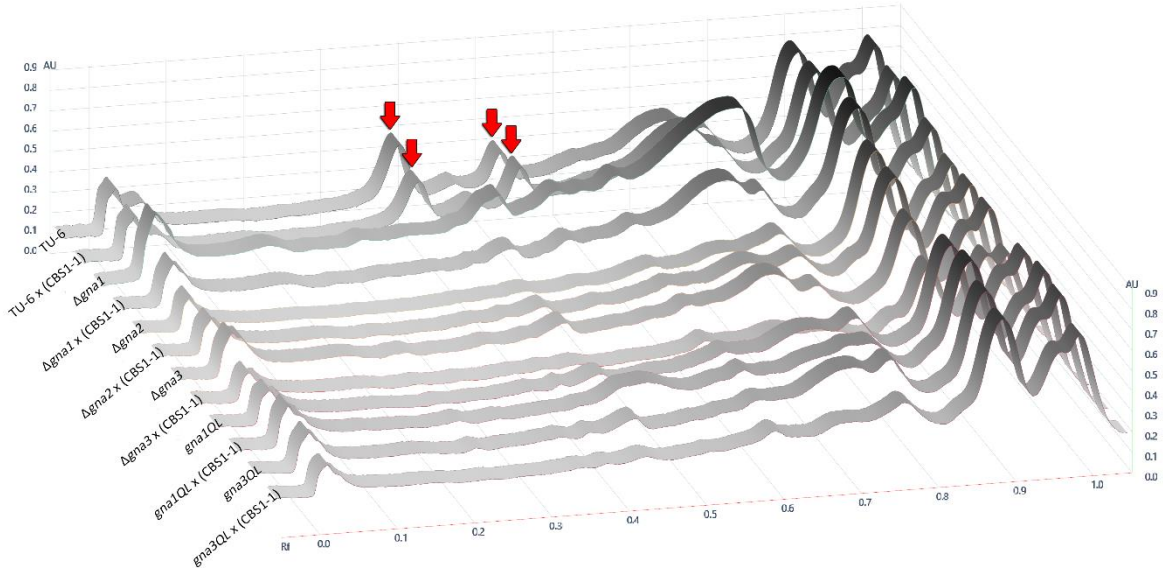

Figure 7. *Scanning densitometry comparison of the secondary metabolite production pattern of T. reesei G-protein α mutant strains under asexual and sexual conditions with the TLC Scanner. See table 1 for sample codes. TU-6 is the corresponding wild type. UV light at 254 nm.*

3.2. G-protein ß and γ subunits

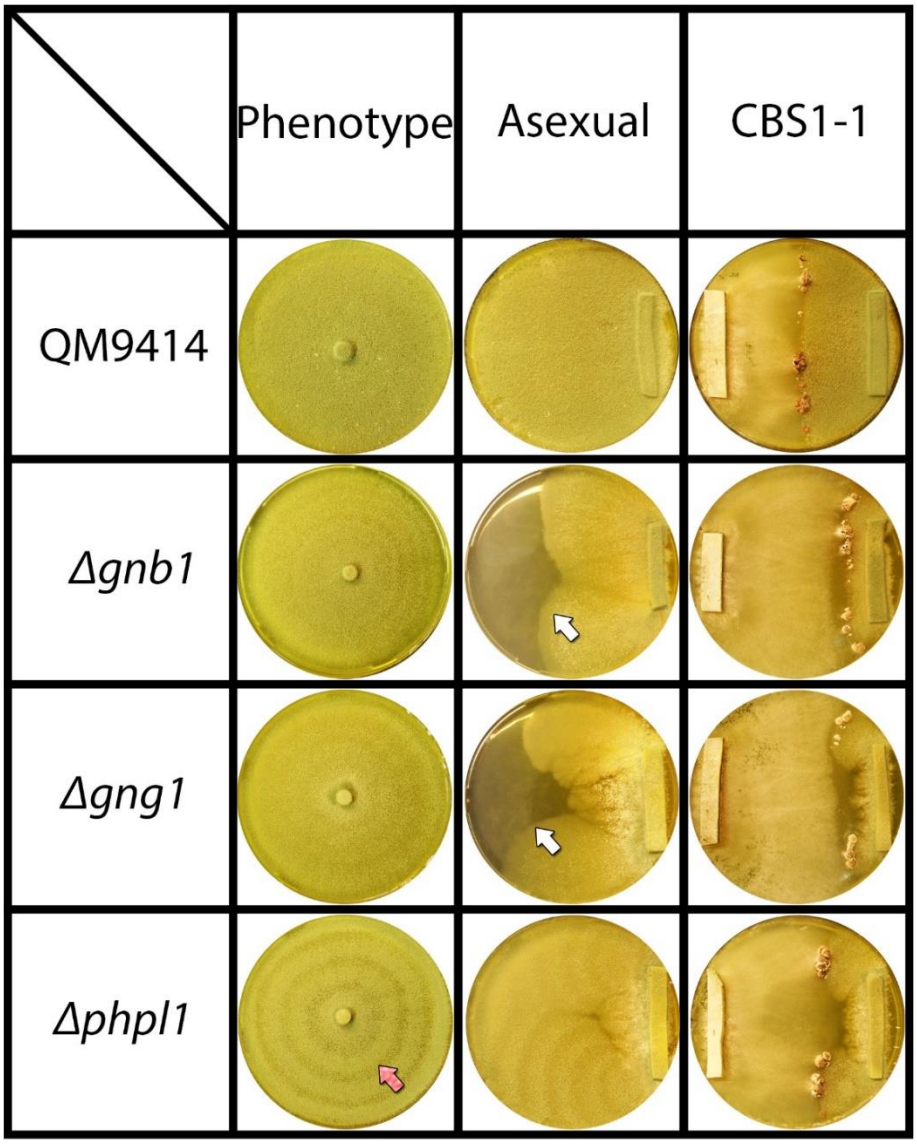

Figure 8. *Phenotype pictures of G-protein ß and γ subunit deletions and deletion of the phosducin-like protein after 2 weeks of inoculation under 22°C, 1700 lux, 12 hours light - 12 hours dark conditions. All the deletion mutations are from the QM9414 background. Strains were grown on 2% (w/v) malt extract agar.*

3.2.1. GNB1 and GNG1 are involved in the regulation of growth

According to the phenotype observations, deletion of G-protein ß subunit GNB1 and G-protein γ subunit GNG1 exhibit similarly reduced biomass formation and these growth patterns are clearly different between the wild type strain and the mutation strains *Δgnb1* and *Δgng1* (Figure 8, Highlighted with white arrows). This finding agrees with the results of Tisch *et al.* (Tisch *et al.*, 2011a).

3.2.2. Deletions of GNB1, GNG1 and PhLP1 display similar sexual development phenotype as the wild type strain

According to the previously published studies from Tisch *et al.*; mutational strains *Δgnb1*, *Δgng1* and *Δphlp1* are able to form fruiting bodies. Furthermore, Tisch *et al.* showed that *Δgnb1* and *Δgng1* mutations do not show important changes in the fruiting body formation in comparison to the parental strain QM9414 (Tisch *et al.*, 2011a).

Our phenotype observations match the findings of Tisch *et al.* regarding the fruiting body formation. *Δgnb1*, *Δgng1* and *Δphlp1* had successful mating with the fully fertile wild type strain CBS999.97 (Figure 8). Concluding that the deletion of the G-protein ß subunit, G-protein γ subunit and the phosducin-like protein PhLP1 don't inhibit the sexual development.

3.2.3. PhLP1 is involved in the conidiation ring formation

The amount of the conidiation rings noticeably decreases below wild type levels upon deletion of the PhLP1 after 14 days of incubation under 12 hours light - 12 hours dark conditions (Figure 8, Highlighted with a red arrow).

3.2.4. GNB1, GNG1 and PhLP1 regulates the chemical communication during sexual development

We tested the response of the metabolite production to the deletions of G-protein ß, γ subunits and PhLP1. HPTLC analysis clearly showed a decrease profile of two compounds if *Δgnb1* or *Δgng1* was one of the mating partners (Figure 9a, Highlighted with white arrows).

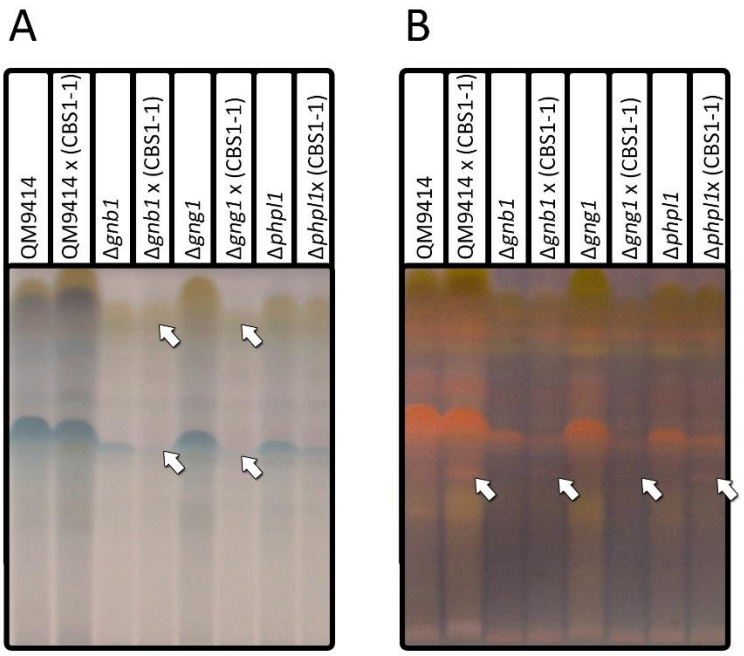

Figure 9. *Secondary metabolite production patterns of T. reesei G-protein ß, γ subunits and PhLP mutant strains under asexual and sexual conditions. See table 1 for sample codes. Different visualisation techniques were applied to detect different substances at each panel and to enable optimal comparison between samples, pictures were reassembled. The corresponding wild type is QM9414.* ***A.*** *Derivatized with anisaldehyde – sulfuric acid, visible light.* ***B.*** *Derivatized with anisaldehyde – sulfuric acid, UV light at 366 nm. Analyses were done in three biological replicates. Replicates were consistent. See supplementary figure 2 for other replicates.*

In response to the deletions of GNB1, GNG1 and PhLP1 secreted secondary metabolites are decreased in comparison to the parental strain QM9414 and the absence of the mating partner decreases the reduction of the secondary metabolite production even more (Figure 9b, Highlighted with white arrows).

3.3. G-protein coupled receptors and pheromones

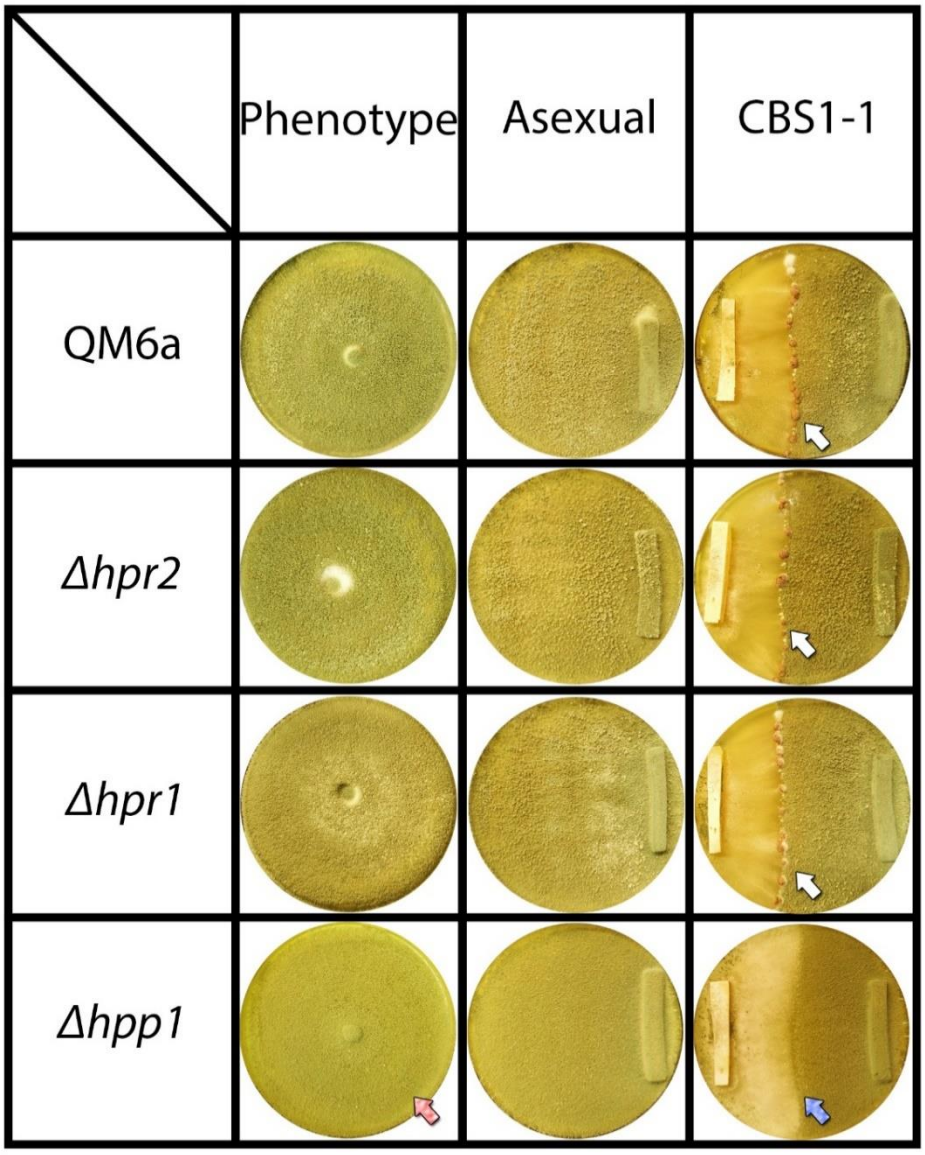

***Figure 10**. Phenotype pictures of G-protein coupled pheromone receptor and pheromone precursor deletions after 2 weeks of inoculation under 22°C, 1700 lux, 12 hours light - 12 hours dark conditions. All the deletion mutations are from the QM6a background. Strains were grown on 2% (w/v) malt extract agar.*

3.3.1. Deletion of G-protein coupled receptors result in a similar phenotype as the wild type strain

Phenotypic observations of the asexual petri dishes of the mutations show that upon deletion of the G-protein coupled receptors HPR1 and HPR2, growth in asexual conditions and conidiation doesn't

seem to be different to the parental strain QM6a (Figure 10). Although there are no obvious phenotypic changes upon deletion of G-protein coupled pheromone precursor HPP1 either, *Δhpp1* strains exhibit less fluffy phenotypes than QM6a (Figure 10, Highlighted a red arrow)

3.3.2. Pheromone precursor HPP1 is required for male fertility

According to the findings of Seidl *et al.*, G-protein coupled pheromone receptors HPR1 and HPR2 are required for female fertility in *T. reesei* (Seidl *et al.*, 2012). Phenotype analysis of the crossings showed that, when the deletion of *hpr1* and *hpr2* are introduced to parental strain QM6a, mutant strains are still able to form fruiting bodies (Figure 10, Highlighted with white arrows). This is because strain QM6a is characterised as female sterile, therefore it acts as a male partner in mating (Seidl *et al.*, 2009). In agreement with earlier reports, our mutant strains *Δhpr1* and *Δhpr2* were able to act as male partners in crossings with the fully fertile wild type CBS999.97.

However, lack of the pheromone precursor HPP1 leads to the abolishment of fruiting body formation, hence an unsuccessful mating (Figure 10, Highlighted with a blue arrow). This means that *Δhpp1* introduces male sterility to the female sterile QM6a, which also agrees with the previous studies (Seidl *et al.*, 2012).

3.3.3. Pheromone system is involved in the regulation of secondary metabolite production

HPTLC analysis revealed that upon deletion of the G-protein coupled pheromone receptors HPR1 and HPR2 and the pheromone precursor HPP1 there were clear differences in the metabolite patterns. Secondary metabolites secreted by receptor mutations *Δhpr1*, *Δhpr2* and *Δhpp1* in the absence of a mating partner were increased compared to the wild type (Figure 11a, Highlighted with white arrows).

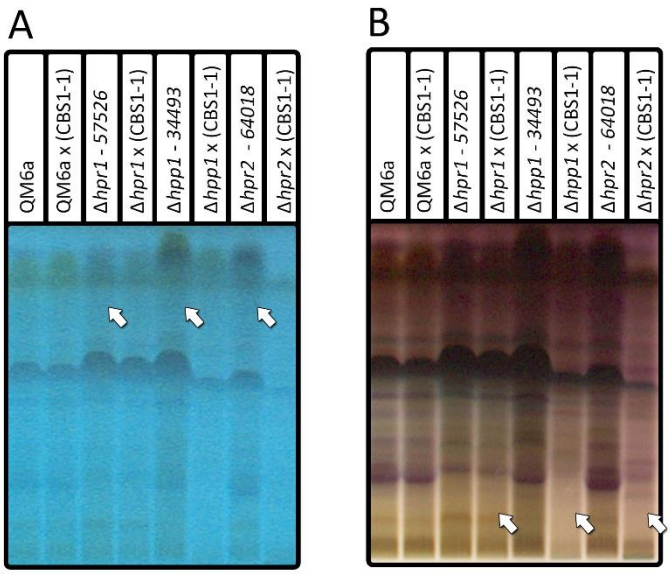

Figure 11. *Secondary metabolite production patterns of T. reesei G-protein coupled pheromone receptors and pheromone precursor strains under asexual and sexual conditions. See table 1 for sample codes. Different visualisation techniques were applied to detect different substances at each panel and to enable optimal comparison between samples, pictures were reassembled. The corresponding wild type is QM6a* ***A.*** *Derivatized with anisaldehyde – sulfuric acid, UV light at 254 nm.* ***B.*** *Derivatized with anisaldehyde – sulfuric acid, visible light. Analyses were done in three biological replicates. Replicates were consistent. See supplementary figure 3 for other replicates.*

Secondary metabolites that are produced by the pheromone receptor mutations and the pheromone precursor mutations are clearly decreased if a potential mating partner was in the vicinity in comparison to those strains that grew alone on the plate (Figure 11b, Highlighted with white arrows). This includes the sorbicilinoid derivative yellow components.

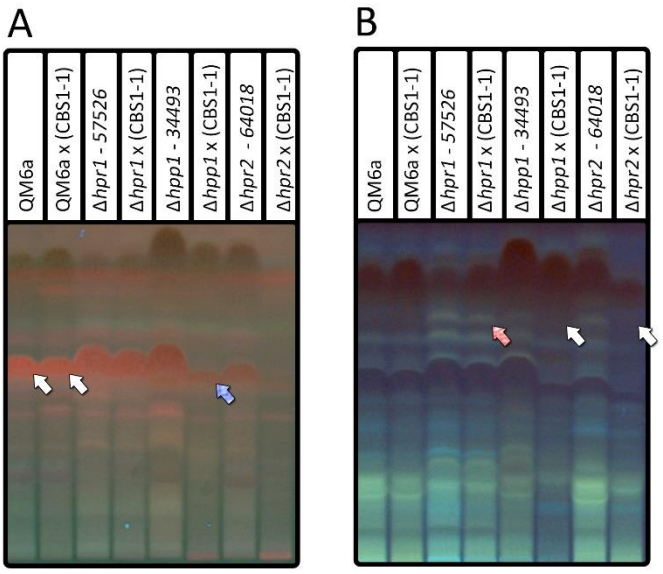

Figure 12. *Secondary metabolite production patterns of T. reesei G-protein coupled pheromone receptors and pheromone precursor strains under asexual and sexual conditions. See table 1 for sample codes. Different visualisation techniques were applied to detect different substances at each panel and to enable optimal comparison between samples, pictures were reassembled. The corresponding wild type is QM6a* ***A.*** *Derivatized with anisaldehyde – sulfuric acid, UV light at 366 nm.* ***B.*** *UV light at 366 nm. Analyses were done in three biological replicates. Replicates were consistent. See supplementary figure 3 for other replicates.*

Apart from the general decrease trend of the secondary metabolite production pattern between the two potential mating partners, some distinct compounds are clearly differently secreted when the mating partner was present. The highlighted compound from the Figure 12a (Highlighted with white arrows) has generally a stable production with the parental strain QM6a and does not alter during sexual development. However, the same compound gets drastically reduced when the strain lacking pheromone precursor gene *hpp1* introduced to a potential mating partner (Figure 12a, Highlighted with a blue arrow).

Another distinct compound with blue fluorescence is produced by the mutational strains in the absence of a mating partner (Figure 12b). This compound is decreased when a potential mating partner is present (Highlighted with white arrows), except the strain that lacks G-protein coupled pheromone receptor HPR1 (Highlighted with a red arrow) (Figure 12b).

4. Discussion

Ascomycete *Trichoderma reesei* was considered asexual for a long time until the discovery of its sexual reproduction recently (Seidl *et al.*, 2009). Therefore, a better understanding of the mechanisms involved in the sexual reproduction of the *T. reesei* became an important subject in the last decade. Sensing the presence of the potential mating partner is a requirement for fungi in order to sustain the successful mating (Schmoll, 2013). Furthermore, recent studies have already shown that this nicely achieved communication with the mating partner is not only set by the pheromones but there were also other secreted compounds involved (Bazafkan *et al.*, 2015). Heterotrimeric G-protein signalling pathway and its pheromone receptors and precursors are essential for the response when a fungus encounters a potential mating partner not only by receiving and transmitting the signal but also by establishing the chemical communication with the partner (Schmoll, 2013; Bazafkan *et al.*, 2015).

The main purpose of this study was to investigate the impact and the importance of the G-protein coupled pheromone signalling machinery during the sexual development in *T. reesei* in terms of chemical communication and to inspect each subunit of the mechanism separately in order to compare their responses when there is a potential mating partner in the vicinity and when they grow alone.

In agreement with the previous findings (Schmoll *et al.*, 2009; Schuster *et al.*, 2012) our study revealed that in *T.* reesei neither the deletion nor the constitutive activation of G-protein α subunits does abolish the sexual development and the fruiting body formation. However, clear differences in the secondary metabolite profile, namely the intensity differences of the bands, suggest that GNAs play a role in the regulation of the chemical communication. Nevertheless, among constitutively activated GNAs and GNA deletions, the secretion of the secondary metabolites don't have a radical difference. Considering constitutive activations of the GNAs are theoretically the opposite of the GNA deficient strains, only having subtle differences is perhaps the result of the complex regulatory factors of the G-protein signalling.

Consistent with the previously reported data (Tisch *et al.*, 2011b), our study also revealed growth defects upon alteration of G-protein ß and γ subunits and the class I phosducin like protein (PhLP1), which is the molecular chaperone of the Gßγ heterodimer. Additionally, our HPTLC data shows a decreased secondary metabolite production pattern upon deletion of the GNB1, GNG1 and PhLP1 both in the absence and presence of a potential mating partner. A possible explanation to this situation could be that functions of GNB1, GNG1 and PhLP1 in *T. reesei* include both; the regulation of the chemical communication and the regulation of the biomass formation.

Furthermore, according to the findings of Seidl *et al.* lack of the pheromone precursor HPP1 introduces male sterility and lack of the pheromone receptors HPR1 and HPR2 introduces female sterility (Seidl *et al.*, 2012). Concurrently, our findings showed that our HPP1 deficient female sterile QM6a strains were not able to mate. However, with HPR1 and HPR2 deficient strains we did not observe such an effect, they were still able to accomplish a successful mating. Due to the fact that in *T.* reesei the absence of one receptor leads to the increased expression of the other pheromone receptor pair (Seidl *et al.*, 2012). Our HPTLC data revealed different secondary metabolite production patterns between sexually and asexually growing cultures. Nonetheless, secretion of the secondary metabolites generally decreases upon the deletion of pheromone receptors and precursor, whether the mating partner is present or not. With this, we could assume that the function of G-protein coupled pheromone signalling is not limited to the signal transition, it extends to chemical communication.

In summary the heterotrimeric G-protein signalling cascade coupled pheromone signalling machinery is a very important signalling pathway for *T. reesei* in terms of generating a "language" to interact and communicate with potential mating partners. This communication does not only consist of the pheromones that are transmitted through the signal transmission network but also consists of the regulation of secreting the metabolites for establishing the chemical communication.

5. Daring to take a step further: Coupling HPTLC with DESI-MS by Blotting

5.1. Introduction to the method

5.1.1. High Performance Thin-Layer Chromatography

Thin-Layer Chromatography (TLC) is a planar separation technique based on the affinity difference of the analyte to the mobile phase and the stationary phase. The mechanism functions, while the mobile phase moves through the stationary phase by the capillary action of the stationary phase, to accomplish the separation of the complex non-volatile mixtures (Fried & Sherma, 1999). High Performance Thin-Layer Chromatography (HPTLC) is a combination of several enhanced features of TLC. These features are; optimization of the plate coating materials, developing the mobile phase and sample application (Costanzo, 1984). HPTLC requires only a little amount of the sample for a rapid,

sensitive and precise analysis which makes it a very useful tool in many scientific fields for potential application of analytical assays (Fenimore & Davis, 1981).

As the name indicates, HPTLC separations take place via development on the thin layer plate, which is an open bed, unlike the other chromatography methods like HPLC, in which the closed column is used for elution. Besides this, with thin-layer chromatography, it is possible to apply the samples multiple times and develop them concurrently. Whereas, at column chromatography samples must be introduced sequentially (Fenimore & Davis, 1981).

5.1.1.1. Stationary and Mobile Phases

A general chromatography system involves two main factors, and these are a stationary phase, which is the adsorbent, and a mobile phase, which is the eluent. A chromatography system works with the application of the solution wherein the sample mixture is present, as mono or multicomponent solutes to the stationary phase. Eventually, the separation occurs on the stationary phase (Grinberg, 1990). The sample solvent passes through the stationary phase with a favoured interaction of the components between the absorbent and the eluent, which will then lead to migration differences between each component (Costanzo, 1984).

5.1.2. Desorption Electrospray Ionization – Mass Spectrometry (DESI – MS)

Mass spectrometry is a commonly used analytical technique in biological and chemical fields due to its significant advantages in sensitivity, speed and specificity (Hu *et al*., 2015). An ambient ionization technique so-called desorption electrospray ionization (DESI) minimizes the pre-treatment of the samples while enabling the analysis on sample's native environment, thus increases the speed of the investigation which makes it superior to other techniques like ESI or MALDI (Shin *et al.*, 2007). This method uses a high-velocity gas jet of charged micro-droplets directed to the surface of the analyte. Then the analyte gets dissolved and extracted by the charged droplets, which are later collected in the MS inlet for analysing (Wiseman & Laughlin, 2007).

5.1.3. Blotting

Despite the mentioned advantages of the HPTLC, a clear determination of the separated compounds is unfortunately not easily possible. Therefore, a combinational approach is required to be able to determine the identity of the separated compounds (Meisen *et al.,* 2011). Coupling HPTLC or TLC with MS offers potential for assaying the samples directly on the HPTLC or TLC plate, where the separation has occurred. This possible capability has drawn a lot of attention, therefore various direct and indirect

coupling methods have already been provided (Hu *et al.,* 2015). One of these methods is the indirect approach, which suggests scrapping or cropping the UV-visible separated bands from the silica plate, followed by the analysis of the extract with soft ionization MS techniques namely ESI and MALDI-MS (Meisen *et al.,* 2004). However, this method comes with a shortcoming: target compound obtained from the silica-coated TLC plate can contaminate the MS instrument with silica particles (Goto-Inoue *et al.,* 2009). Observing the analytes on a TLC plate directly with the MS coupled ionization methods are beneficial in terms of reducing the sample preparation time, yet these direct ionization methods are inadequate as well, due to the irregular surface properties of the silica gel which reduces the accuracy of the mass spectrometry (Meisen *et al.,* 2011). Nevertheless, as a modification of the predecessor technique, which uses the principles of the direct analysis; transferring the separated sample to a PVDF membrane by TLC blotting was introduced by Taki *et al.* with the name of Far-Eastern blotting (Ishikawa & Taki, 2000). Far-Eastern blotting suggests building a blotting assembly and pressing this assembly with a 180°C iron (Ishikawa & Taki, 2000). However, using such a high temperature for the application reduces the feasibility of the method in various fields, including temperature-sensitive biological samples. In this study, we have developed successfully a method which is easier to handle, and it can hold up a more comprehensive sample selection.

5.2. Materials and Methods

One of the most favourable planar chromatography method, HPTLC, is a subcategory of liquid chromatography, which works with capillary forces between the liquid mobile phase and the stationary phase. A thin layer on a flat plate is used as a stationary phase in the planar chromatography. The migration of the components occurs due to the conflict between the driving force of the mobile phase, that tends to move the substances in the direction of the flow and the resistive action of the stationary phase, which holds the substances back onto the sorbent; hence individual components of the samples migrate at a certain distance (Fried & Sherma, 1999).

5.2.1. Stationary phase

Silica gel with its polar surface properties is the most commonly used coating material for the HPTLC plates (Gocan, 2002). The performance of the stationary phase is mostly determined by pore sizes and pore distributions of the silica gel (Costanzo, 1984). Due to its adsorptive properties, silica serves as a selective sorbent and when it's purified properly, it has no tendency to catalyse a reaction with the components of the substances apart from acidic cleavage (Fried & Sherma, 1999).

As the stationary phase, we have mostly used silica gel coated aluminium high-performance thin-layer chromatography plates with a fluorescent indicator (HPTLC plate, silica gel 60, E. Merck, Darmstadt, Germany).

5.2.2. Tracer dyes

Being an open system, HPTLC permits a simultaneous development of multiple samples according to their polarity properties. Polar substances interact strongly with the polar stationary phase and thus remain near to the origin in comparison to nonpolar substances, which interact weakly with the surface and get moved away by the mobile phase (Fenimore & Davis, 1981).

To understand the influence between the TLC plate (stationary phase), dyes (samples) and the eluent (mobile phase), we have chosen seven different dyes with different polarity properties to cover a wide polarity range (Table 2).

Apart from some of the refinement tests, which were done by the Automatic TLC Sampler, we have mostly used a conventional glass capillary pipet to manually spot the dyes on silica plates.

Table 2. *List of the chosen dyes for experiments. Listed from more-polar to less-polar.*

Dye	Name	Chemical Formula	CAS number
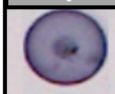	Reactive Black	$(C_{26}H_{21}N_5Na_4O_{19}S_6)$	17095-24-8
	Brilliant Green	$(C_{27}H_{33}N_2HO_4S)$	633-03-4
	Rhodamine B	$(C_{28}H_{31}ClN_2O_3)$	81-88-9
	Disperse Black	$(C_{16}H_{20}N_4O_2)$	6054-48-4
	Fluorescein	$(C_{20}H_{12}O_5)$	2321-07-05
	Chrysazin	$(C_{14}H_8O_4)$	117-10-2
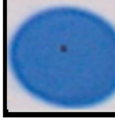	Unisol Blue	$(C_{20}H_{22}N_2O_2)$	14233-37-5

5.2.3. Blotting solvent

In addition to the sensitivity and polarity parameters, another important criterion for compound separation through HPTLC is the selectivity of the solvent. Selectivity is based on slight differences in interactions between the mobile phase and the compounds (Lesellier, 2015).

With all these parameters taken into account, we have tested the developing process of each chosen dye, mentioned above, with numerous solvents. Furthermore, we have mixed specific solvents with each other with the focus on the limiting parameters, especially the selectivity and viscosities of the solvents and eventually, we have chosen the azeotropic ethanol/toluene (68:32% by weight) mixture to be the best solvent for our blotting approach.

5.2.4. Blotting supplements

The capillary phenomenon is the processing mechanism of the separation through an HPTLC plate. In Far Eastern blotting, transferring the separated samples from HPTLC plate to a membrane with blotting analyses is also relying on the same approach: the component is transferred to the blotting membrane via the capillary action of the solvent and the adsorbent layer above the sample (Taki & Ishikawa, 1997; Barden, 2013).

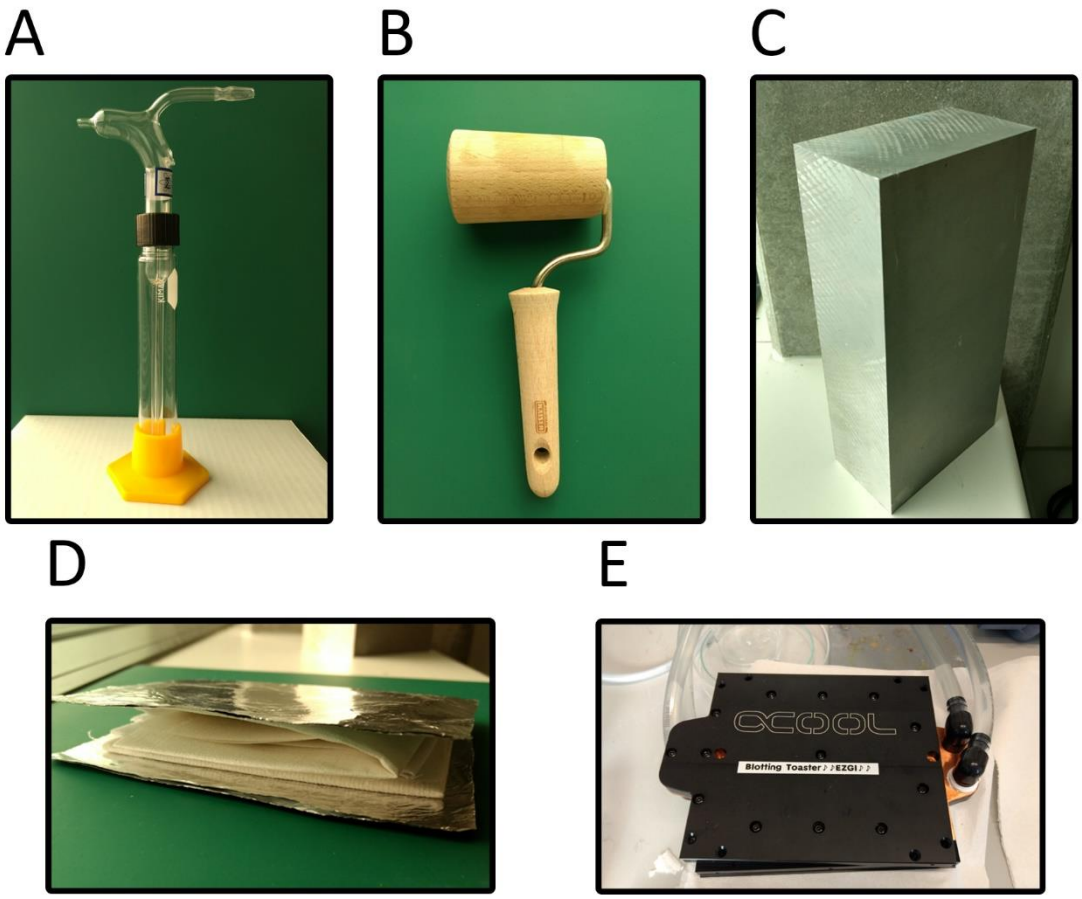

Figure 13. *Supplementary materials for blotting.* ***A.*** *Tube type sprayer,* ***B.*** *Roller,* ***C.*** *Aluminium weight,* ***D.*** *Blotting sandwich in the aluminium envelope,* ***E.*** *Blotting thermostat ("toaster")*

Our experiments, in brief, were as follows: After the separation on the silica plate, we wetted the developed HPTLC plate with our solvent of choice, mentioned on chapter 5.2.3., azeotropic ethanol/toluene while utilizing a tube-type sprayer with a reservoir greater than 10 ml (Figure 13a). Immediately after delicately coating the HPTLC plate with azeotropic ethanol/toluene, nanofibrillated cellulose (NFC) was placed as a blotting membrane on top of the silica plate carefully to avoid the generation of air bubbles in between.

Based on the capillary action principle of blotting, we have used a stack of filter paper to cover the membrane so that the capillary action of the adsorbent layer was enhanced with the support of the filter paper stack. This entire sandwich was then transferred into a pre-prepared aluminium envelope instantaneously (Figure 13d). The aluminium envelope is used to support the stack without isolating the heat transfer and it was made by simply folding a piece of aluminium foil into two.

Lastly, we have used a pastry roller not only to fix the sandwich but also to make the aluminium foil unwrinkled to avoid uneven blotting (Figure 13b).

Eventually, we placed the sandwich in the preheated blotting toaster, which contains two heating plates (Figure 13e). Both heating plates were connected to a circulating water bath with temperature control to keep the temperature of the plates stable.

For successful blotting, we supported the plates with an aluminium block approximately 6 kg in weight (Figure 13c). The point of this weight was to be able to apply equal pressure on the entire plate and to make the blotting more adequate.

Lastly, the blotting was done at 40°C in 10 minutes.

After 10 minutes of blotting, a copy of the sample had been transferred to the nanofibrillated cellulose nicely and this silica-free duplication of the sample was ready to be analysed with DESI-MS without the need for further treatment (Figure 14e).

5.3. Results and Discussion

5.3.1. Blotting membranes

One of the most crucial parts of blotting is choosing the membrane which will represent the surface for transferring the samples from the HPTLC plate. For successful blotting, the membrane needs to fulfil multiple criteria. Firstly, it must have certain absorbability in order to have the mirroring image on itself. It should be stable under the blotting conditions. It should also be relatively pure to prevent problems with DESI. To obtain robust results from DESI-MS, the distance between the device and the surface bearing the analyte must be kept constant. In other words, a smoother membrane will provide better images than one with a complex surface topography in terms of spatial resolution (Nguyen *et al.*, 2017). Lastly, easy application and availability of the prospective membrane would be advantageous.

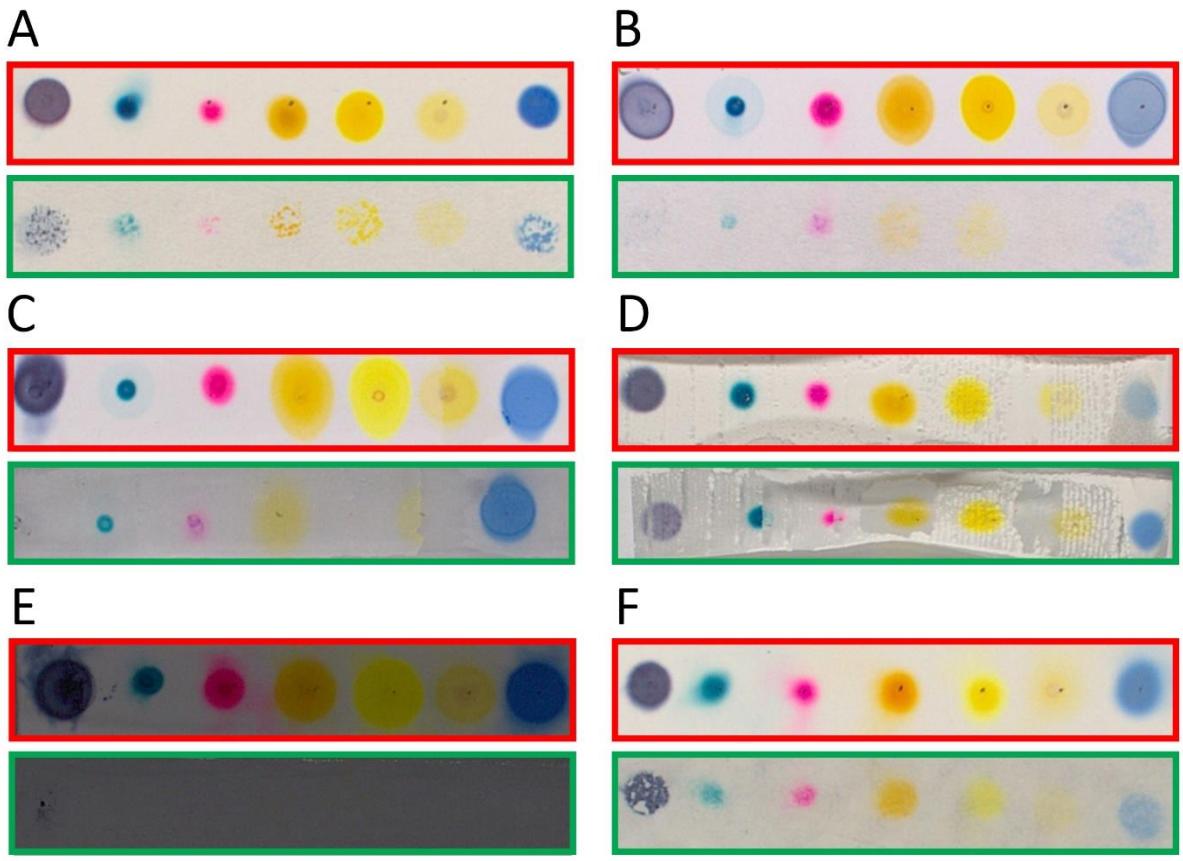

Figure 14. *Various membranes tested for successful blotting. (Red rectangles indicate HPTLC plates after botting. Green rectangles indicate blotted membranes.)* ***A. Filter paper;*** *low level of smearing on the HPTLC plate, the clear mirroring image on itself due to its sorption properties. High level of mottled blotting due to its rough surface.* ***B. Chromatography paper;*** *low level of smearing on the HPTLC plate due to its sorption properties. A lower level of mottled blotting (in comparison to the filter paper) due to its less rough surface. The faded mirroring image on itself.* ***C. Tesa™ tape;*** *a clear mirroring image on itself due to its sticky properties and smooth surface. Silica layer gets stuck on the tape because of the glue.* ***D. Scotch™ tape;*** *a clear mirroring image on itself due to its sticky properties and smooth surface. Lower heat resistance. Silica layer gets stuck on the tape because of the glue.* ***E. Cellophane;*** *high level of smearing and weak blotting due to its low sorption properties.* ***F. Nanofibrillated cellulose;*** *low level of smearing, neat blotting.*

We have analysed various kinds of membranes such as filter paper, which has a very high level of absorbance. However, its rough surface properties caused a mottled image after blotting (Figure 14a). Smoother chromatography paper has reduced the mottling effect as well as the clear mirroring image on itself (Figure 14b). Further, we have tested multiple brands of sticky tapes to minimise the sliding of the membrane to improve the transfer (Figure 14c and d). Although blotted dyes were clear and easy to identify, the glue on the tape was ripping a tiny layer of silica from the HPTLC plate, making it very risky to further analyse with DESI. Additionally, they were not always heat resistant, which is required for blotting. Cellophane, a very smooth yet not absorbent form of cellulose, was causing a high level of smearing on the HPTLC plate alongside with weak blotting (Figure 14e).

After testing various membranes, we have chosen the nanofibrillated cellulose (NFC). In the last decades, nanofibrillated cellulose is drawing attention not only because of the nanosized dimension of its fibres but also due to its outstanding strength and flexibility (Martins *et al.*, 2010). To that end, it made a remarkable candidate for our blotting assembly because of its perfectly smooth surface for coupling with DESI-MS (Figure 14f).

5.3.2. Solvent treatment

Based on the capillary principle, we needed to choose a solvent and a solvent application method to transfer the tracer dyes from the HPTLC plate to a membrane with the help of the solvent of choice. In the first instance, we treated the HPTLC plate by simply immersing it in the solvent, which resulted in severe dispersion (Figure 15a). Immersing the nanofibrillated membrane instead of the plate before blotting however didn't cause as much dispersion as immersing the HPTLC plate, yet the edges of the samples were not nicely defined.

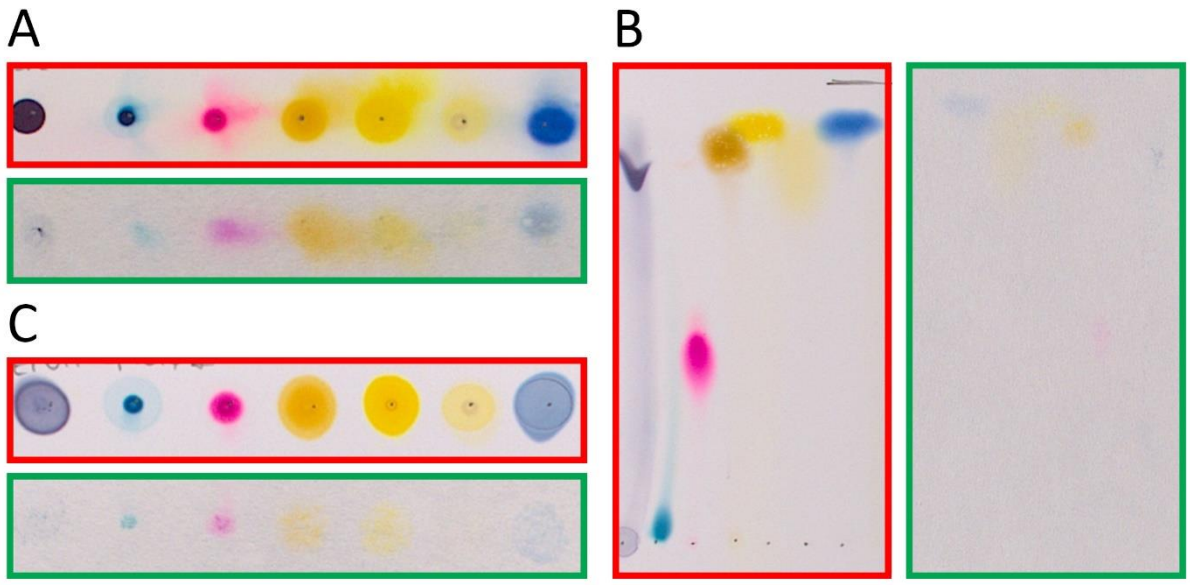

Figure 15. *Various solvent application techniques to HPTLC plate for blotting. (Red rectangles indicate HPTLC plates after botting. Green rectangles indicate blotted membranes.)* ***A.*** *Immersing HPTLC plate into the solvent for blotting causes a high level of smearing.* ***B.*** *Instantaneous blotting after developing causes a low level of smearing.* ***C.*** *Spraying the HPTLC plate gives the user to control the solvent amount to avoid smearing.*

As an alternative, we have tested instantaneous blotting after developing the samples, when the plate was still wet from development. Not adding extra solvent to treat the HPTLC plate was a nice alternative in terms of the durability of the plate. However, putting blotting as an additional step between developing and scanning was not convenient and feasible when one needed sensitive scanning results, due to the fact that the blotting results in slight dispersion, because of the compression of the membrane (Figure 15b).

Lastly, we have tried spraying the solvent on the membrane and to the silica plate. Zarzycki and Zarzycka demonstrated that using the sprayer generates small-scaled droplets for homogenous coverage of the HPTLC plate (Zarzycki & Zarzycka, 2008). Spraying the azeotropic ethanol/toluene directly on the HPTLC plate by using an amount that just made it slightly glistening wet was the best method among the others for its feasibility in terms of handling both the membrane and the plate as well as visualising sharply defined blotted images (Figure 15c).

5.3.3. Adjusting the conditions for blotting

Blotting the samples to the nanofibrillated cellulose by spraying the HPTLC plate with azeotropic ethanol/toluene is an uncomplicated procedure. For the repeatability and usefulness of the application, viable and optimal conditions needed to be determined.

5.3.3.1. Temperature and duration

In order to obtain robust data and determine the optimum temperature, we have tested the temperature range between 40°C to 80°C in ten-degree steps as well as the time range between one minute to 30 minutes in five-minute steps in several permutations while baking the blotting heap in the oven (Figure 16). Hence, we could say that elevating the temperature increases the quality of blotting (Figure 16a to d). However, when temperature-sensitive samples are taken into account, such high temperatures would disturb the samples. Therefore, increasing the duration of blotting rather than the temperature would increase the feasibility of the method. Besides, as it is shown in figure 16e and f, doubling the duration increases the quality of blotting more than doubling the temperature. Consequently, we have decided that warming up the samples to 40°C for 10 minutes is the best condition to achieve good quality.

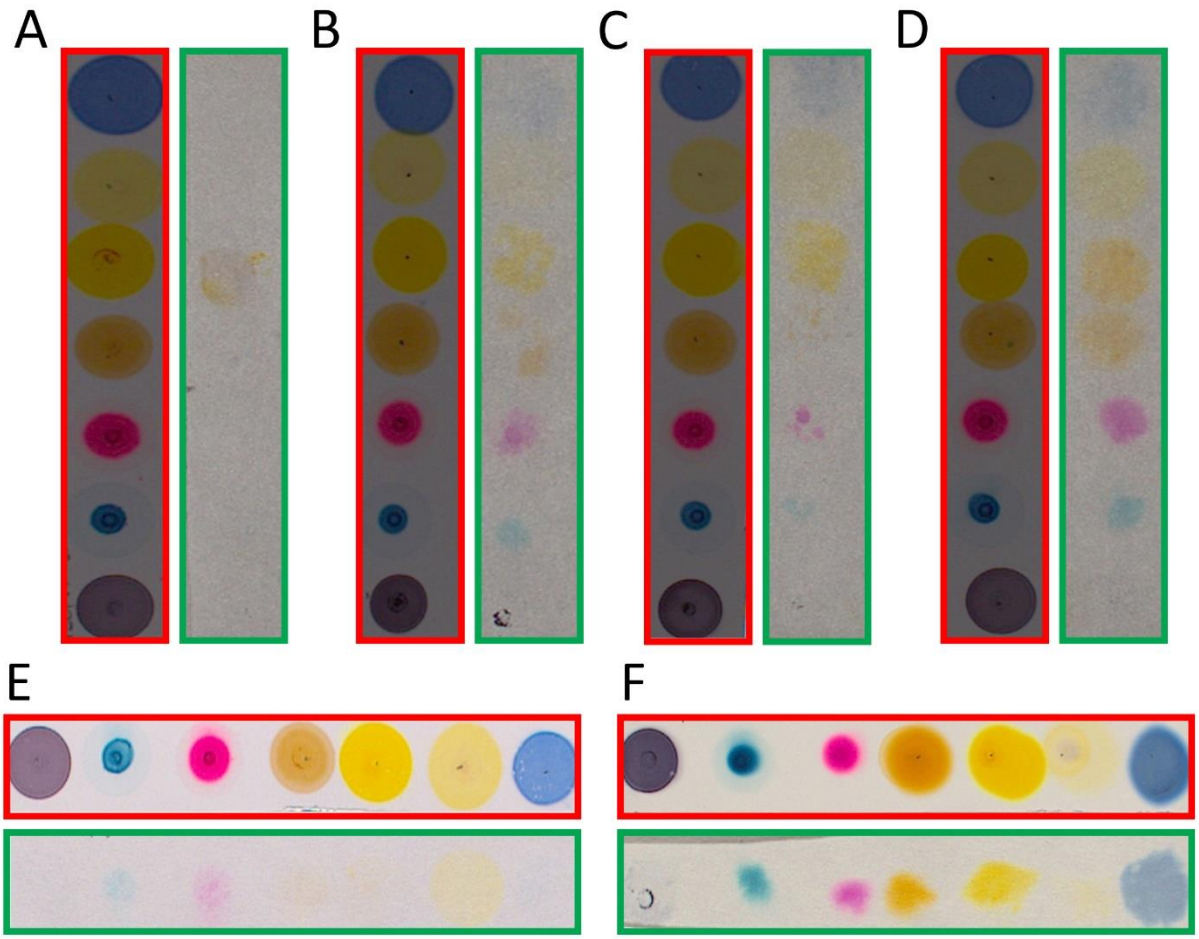

Figure 16. *Temperature and time series for optimization. Increasing temperature and time increases the quality of blotting. (Red rectangles indicate HPTLC plates after botting. Green rectangles indicate blotted membranes.)* ***A.*** *Blotting at 50°C for 3 minutes.* ***B.*** *Blotting at 60°C for 3 minutes.* ***C.*** *Blotting at 70°C for 3 minutes.* ***D.*** *Blotting at 80°C for 3 minutes.* ***E.*** *Blotting at 80°C for 5 minutes.* ***F.*** *Blotting at 40°C for 10 minutes.*

Initially, we used an oven to warm up our samples for blotting. However, incubating in an oven had its shortcomings. Blotting must be done in the fume hood, for security measures, to avoid the inhalation of the sprayed chemicals. Therefore, it was not convenient to carry the blotting sandwich from the hood to the oven, because of the increased incubation time at room temperature. Furthermore, blotting in the oven was not an environmentally friendly solution for increasing the temperature, considering the lost heat while placing the blotting set inside of the oven, and the energy required for heating up a large oven for small-sized blotting.

Hence, we have constructed a 'blotting toaster' using copper-coated heating plates with isolation at one side. We have connected the heating plates to a circulating warm water bath with temperature control, in order to heat the toaster rapidly and keep the temperature stable, while increasing the isolation capacity (Figure 13e).

It took only five minutes for the circulating water bath to warm up the plates of the toaster from room temperature to 40°C. Additionally, as a result of being connected to the heating plates, one could define the precise temperature of the blotting process. Consequently, the blotting toaster was easier to handle, it provided constant temperature and eventually efficient blotting.

5.3.4. HPTLC applications

In order to determine the usefulness of blotting with an entire HPTLC plate, we have run several experiments using the whole HPTLC setup, including; Automatic TLC sampler (ATS4), Automatic Development Chamber (ADC2), Visualizer, Scanner 3.

5.3.4.1. Concentration Series

Quantitative determination of the viable concentrations of the tracer dyes allows us to select the lowest concentration for the blotting.

Figure 17. *HPTLC sampling of the tracer dyes to determine the optimal concentration*

In consideration of covering an extensive concentration range, we have dissolved and diluted each dye to eight different concentrations from C=1000µg/ml to C=0,3µg/ml and sprayed 2µl from each one of them onto an HPTLC plate by using ATS4 (Figure 17).

After the sample application step, we have performed the blotting of the entire HPTLC at 40°C for 10 minutes. Consequently, with the mirroring image of the blotted sample on the membrane (Figure 18), we could determine that with the method, even the lower concentrations can be transferred to the membrane.

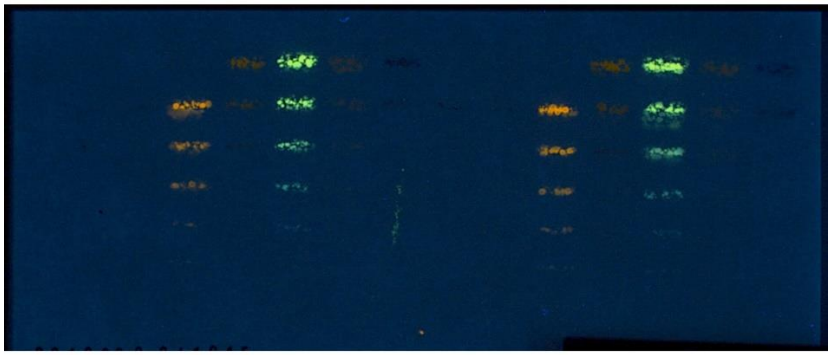

Figure 18. *The blotted membrane of concentration series under the UV light at 366 nm. After blotting some dyes were visually detectable even at the concentration of 3,3µg/ml.*

5.3.4.2. Peak broadening

In terms of obtaining maximum signal intensities with DESI-MS, it must be considered that the zone concentration of the blotted component and the size of the zone play important roles (Morlock & Schwack, 2010). To be able to correlate the difference between before and after blotting in terms of concentration and size, we needed to figure out the amount of dispersion by comparison.

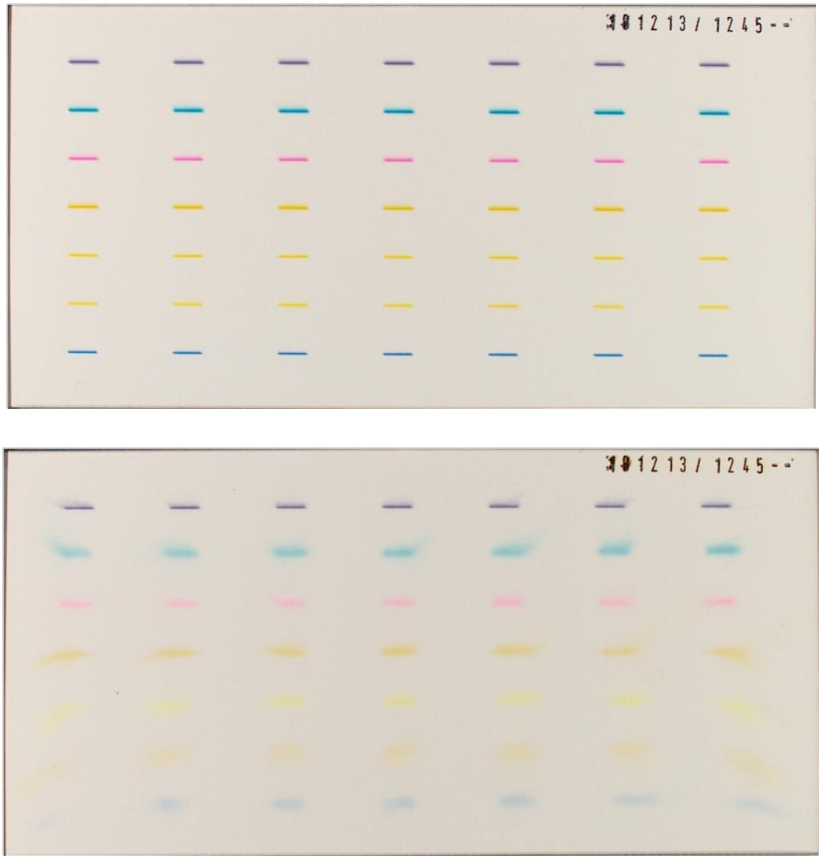

Figure 19. *Top: HPTLC sampling of the tracer dyes to determine the dispersion of the dyes. Bottom: After blotting the same silica plate.*

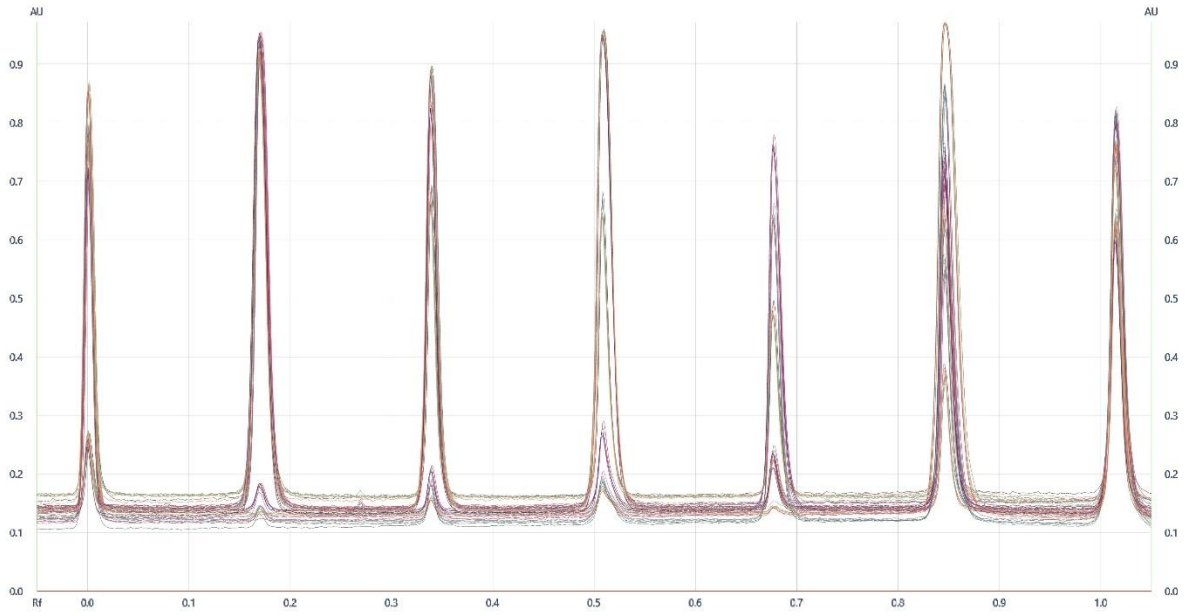

Figure 20. *Scanning of the HPTLC chromatogram at seven different wavelengths before blotting.*

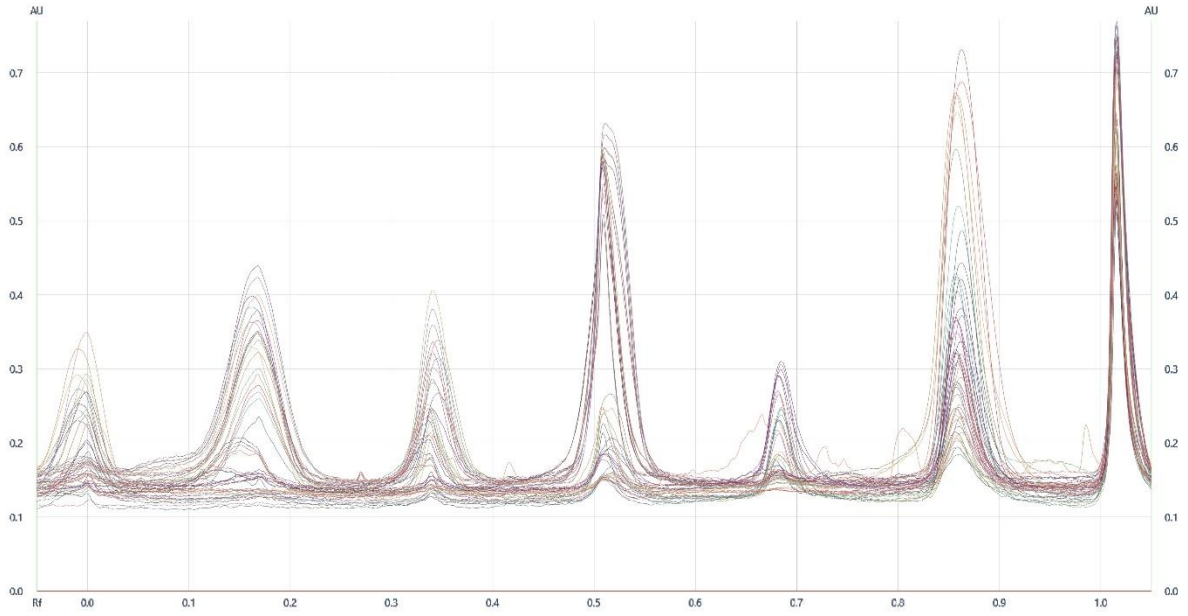

Figure 21. *Scanning of the same HPTLC chromatogram at same wavelengths after blotting.*

We initially sprayed the plate with each dye at a certain concentration using the automatic TLC sampler (Figure 19). Before blotting, we scanned the plate at seven different wavelengths to obtain the graphical data (Figure 20). Thereafter we blotted the plate with the mentioned method and

scanned the plate once more with the same setting, to obtain graphical data from the same samples after blotting, for comparison (Figure 21).

Scanning results indicate that while some dye zones remained quite intact, others dispersed and lost their intensity. Nevertheless, this issue can be minimized with further optimization of the spraying step with alterations of pressure properties, or even with the adjustments of user-dependent properties, like the holding angle of the sprayer and its distance to the silica plate.

5.3.4.3. Two Dimensional HPTLC

Two dimensional (2D) HPTLC is used to increase the resolution of the separation during the investigation of a substance from a complex mixture. 2D HPTLC uses the principle of perpendicularly changing the flow direction between two sequential developments with different mobile phases so that the entire surface of the plate is used for separation (Fenimore & Davis, 1981). Although conventional HPTLC can be used for separation of many samples, 2D HPTLC allows only to separate more complex samples. By using the entire surface of the plate for single sample separation, one can obtain almost squared resolving power in comparison to the standard mono-dimensional HPTLC, as the peak capacities of each separation are multiplied (Fenimore & Davis, 1981).

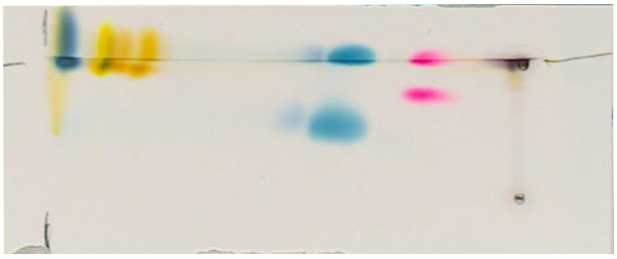

Figure 22. *2-Dimensional separation of the dyes. 1D - EtOH:Toluene (1:1), 2D MeOH:Hexane (4:1)*

To acquire the feasibility of the blotting application after the two-dimensional separation of the HPTLC plate, we have arranged various mixtures of our chosen tracer dyes at different concentrations. Using these mixtures, we have assayed them with a various solvent selection which we have been using for mono dimensional HPTLC and additionally, we have also used several solvent mixtures according to their miscibility properties with each other, thus we have selected two solvent mixtures as mobile phases of our 2D HPTLC approach. The solvent mixture Ethanol:Toluene (1:1 – V:V) was used for the

first dimension and the solvent mixture Methanol:Hexane (4:1 – V:V) was used for the second dimension. These two solvent mixtures could separate the dye mixture neatly (Figure 22).

Eventually, after the separation on the silica plate, we have applied our blotting method to the multidimensionally developed substances. 2D HPTLC results in more selective separation in comparison to the standard HPTLC, meaning that the components get separated more distinctively. Considering this benefit, we have indeed accomplished successful blotting, which was proof of the feasibility of our blotting method in collaboration with 2D HPTLC.

In summary, we were able to introduce a user-friendly method to analyse the samples, that are already separated by the HPTLC, with mass spectrometry. Our blotting method can be used with awide range of samples in terms of polarity and temperature sensitivity. Besides this, instead of tedious sample preparations for mass spectrometry, quick blotting with inexpensive instruments gives a big advantage to our blotting method, which is still being improved by our laboratory. Therefore, it offers a big potential for the identification of the distinct compounds from complex samples, including the secreted metabolites from *T. reesei*.

6. References

Barden D. (2013) Southern blotting. In *Brenner's Encyclopaedia of Genetics 2nd Edition*. Maloy S., Hughes K. (eds). Academic Press, pp. 492-493

Bayram Ö., Braus G. H. (2012) Coordination of secondary metabolism and development in fungi: the velvet family of regulatory proteins. *FEMS Microbiol. Reviews* 36: 1-24.

Bazafkan H., Beier S., Stappler E., Böhmdorfer S., Oberlerchner J. T., Sulyok M., Schmoll M. (2017) SUB1 has photoreceptor dependent and independent functions in sexual development and secondary metabolism in *Trichoderma reesei*. *Molecular Microbiology* 106(5): 742-759.

Bazafkan H., Dattenböck C., Böhmdorfer S., Tisch D., Stappler E., Schmoll M. (2015) Mating type dependent partner sensing as mediated by vel1 in *Trichoderma reesei. Molecular Microbiology* 96(6): 1103-1118

Bischof R. H., Ramoni J., Seiboth B. (2016) Cellulases and beyond: the first 70 years of the enzyme producer *Trichoderma reesei*. *Microbial Cell Factories* 15: 106

Busch S., Braus G. H. (2007) Micro commentary: how to build a fungal fruit body: from uniform cells to specialized tissue. *Molecular Microbiology* 64(4): 873-876

Cardoza R. E., Hermosa M. R., Vizcaíno J. A., Sanz L., Monte E., Gutiérrez S. (2015) secondary metabolites produced by *trichoderma* and their importance in the biocontrol process. *Microorganisms for Industrial Enzymes and Biocontrol* 37(2): 1-22

Costanzo S. J. (1984) High performance thin-layer chromatography. *Journal of Chemical Education* 61(11): 1015-1018

Dattenböck C., Tisch D., Schuster A., Monroy A. A., Hinterdobler W., Schmoll M. (2018) Gene regulation associated with sexual development and female fertility in different isolates of *Trichoderma reesei*. *Fungal Biology and Biotechnology* 5: 9

Druzhinina I. S., Kopchinskiy A. G., Kubicek C. P. (2006) The first 100 *Trichoderma* species characterized by molecular data. *Mycoscience* 47: 55-64

Fenimore D. C., Davis C. M. (1981) High performance thin-layer chromatography. *Analytical Chemistry* 53(2): 252-266

Fried B., Sherma J. (1999) Thin-layer chromatography, fourth edition, revised and expanded. New York: CRC Press

Gerlach A. D. C. L., Gadea A., Silveira R. M. B. D., Clerc P., Dévéhat F. L. (2018) The use of anisaldehyde sulfuric acid as an alternative spray reagent in TLC analysis reveals three classes of compounds in the genus *Usnea* Adans (Parmeliaceae, lichenized Ascomycota). *Preprints* doi: 10.20944

Gocan S. (2002) Stationary phases for thin-layer chromatography. *Journal of Chromatographic Science* 40: 1-12

Goto-Inoue N., Hayasaka T., Taki T., Gonzalez T. V., Setou M. (2009) A new lipidomics approach by thin-layer chromatography-blot-matrix-assisted laser desorption/ionization imaging mass spectrometry for analyzing detailed patterns of phospholipid molecular species. *Journal of Chromatography A* 1216: 7096-7101

Grinberg N. (1990) Modern thin-layer chromatography. New York: Marcel Dekker, Inc.

Gruber F., Visser J., Kubicek C. P., de Graaff L. H. (1990) The development of a heterologous transformation system for the cellulolytic fungus *Trichoderma reesei* based on a pyrG-negative mutant strain. *Current Genetics* 18: 71-76

Gruber S., Omann M., Zeilinger S. (2013) Comparative analysis of the repertoire of G-protein-coupled receptors of three species of the fungal genus *Trichoderma*. *BMC Microbiology* 13:108

Heitman J., Sun S., James T. Y. (2013) Evolution of fungal sexual reproduction. *Mycologia* 105: 1-27

Harman G. E., Howell C. R., Viterbo A., Chet I., Lorito M. (2004) *Trichoderma* species – opportunistic, avirulent plant symbionts. *Nature Reviews – Microbiology* 2: 43-56

Hinterdobler W., Schuster A., Tisch D., Özkan E., Schinnerl J., Brecker L., Böhmdorfer S., Schmoll M. (2019) The role of PKAc1 in gene regulation and trichodimerol production in *Trichoderma reesei*. *Fungal Biology and Biotechnology* 6:12

Hu B., Xin G. Z., So P. K., Yao Z. P. (2015) Thin layer chromatography coupled with electrospray ionization mass spectrometry for direct analysis of raw samples. *Journal of Chromatography A* 1415: 155-160

Ishikawa D., Taki T. (2000) Thin-layer chromatography blotting using polyvinylidene difluoride membrane (Far-Eastern Blotting) and Its Applications. *Methods in Enzymology* 312: 145-157

Kubicek C. P., Komon-Zelazowska M., Druzhinina I. S. (2008) Fungal genus *Hypocrea/Trichoderma*: from barcodes to biodiversity. *Journal of Zhejiang University SCIENCE B* 9(10): 753-763

Lesellier E. (2015) Σpider diagram: a universal and versatile approach for system comparison and classification – application to solvent properties. *Journal of Chromatography A* 1389: 49-64

Li L., Wright S. J., Krystofova S., Park G., Borkovich A. (2007) Heterodimeric G-protein signalling in filamentous fungi. *Annual Reviews of Microbiology* 61: 423-452

Martinez D., Berka R. M., Henrissat B., Saloheimo M., Arvas M., Baker S. E., *et al.* (2008) Genome sequencing and analysis of the biomass-degrading fungus *Trichoderma reesei* (syn. *Hypocrea jecorina*). *Nature Biotechnology* 26: 553-560

Martins N. C. T., Freire C. S. R., Pinto R. J. B., Fernandes S. C. M., Neto C. P., Silvestre A. J. D., Causio J., Baldi G., Sadocco P., Trindade T. (2012) electrostatic assembly of Ag nanoparticles onto nanofibrillated cellulose for antibacterial paper products. *Cellulose* 19: 1425-1436

Meisen I., Mormann M., Müthig J. (2011) Thin-layer chromatography, overlay technique and mass spectrometry: a versatile triad advancing glycosphingolipidomics. *Biochimica et Biophysica Acta* 1811: 875-896

Meisen I., Peter-Katalinić J., Müthing J. (2004) direct analysis of silica gel extracts from immunostained glycosphingolipids by nanoelectrospray ionization quadrupole time-of-flight mass spectrometry. *Analytical Chemistry* 76(8): 2248-2255

Morlock G., Schwack W. (2010) Coupling of planar chromatography to mass spectrometry. *Trends in Analytical Chemistry* 29(10): 1157-1171

Nguyen S. N., Liyu A. V., Chu R. K., Anderton C. R., Laskin J. (2017) Constant-distance mode nanospray desorption electrospray ionization mass spectrometry imaging of biological samples with complex topography. *Analytical Chemistry* 89: 1131-1137

Samuels G. J. (1996) *Trichoderma*: a review of biology and systematics of the genus. *Mycological Research* 100(8): 923-935

Schmoll M. (2008) The information highways of a biotechnological workhorse – signal transduction in *Hypocrea jecorina*. *BMC Genomics* 9: 430

Schmoll M. (2013) Sexual development in *Trichoderma* – scrutinizing the aspired phenomenon. In *Trichoderma: Biology and Applications*. Mukherjee P. K., Horwitz B. A., Singh U. S., Mukherjee M., Schmoll M. (eds). Oxfordshire, UK: CAB International, pp. 67-86

Schmoll M, Esquivel-Naranjo E. U., Herrera-Estrella A. (2010) *Trichoderma* in the light of day – physiology and development. *Fungal Genetics and Biology* 47: 909-916

Schmoll M, Schuster A., Silva R. D. N., Kubicek C. P. (2009) The G-Alpha protein GNA3 of *Hypocrea jecorina* (anamorph *Trichoderma reesei*) regulates cellulase gene expression in the presence of light. *Eukaryotic Cell* 8(3): 410-420

Schuster A., Bruno K. S., Collett J. R., Baker S. E., Seiboth B., Kubicek C. P., Schmoll M. (2012) A versatile toolkit for high throughput functional genomics with *Trichoderma reesei*. *Biotechnology for Biofuels* 5:1

Schuster A., Schmoll M. (2010) Biology and biotechnology of *Trichoderma*. *Applied Microbiology and Biotechnology* 87(3): 787-79

Seibel C., Gremel G., Silva R. D. N., Schuster A., Kubicek C. P., Schmoll M. (2009) Light-dependent roles of the G-protein α subunit GNA I of *Hypocrea jecorina* (Anamorph *Trichoderma reesei*). *BMC Biology* 7:58

Seibel C, Tisch D., Kubicek C. P., Schmoll M. (2012) The role of pheromone receptors for communication and mating in *Hypocrea jecorina* (*Trichoderma reesei*). *Fungal Genetics and Biology* 49(10): 814-824

Seidl V., Seibel C., Kubicek C. P., Schmoll M. (2009) Sexual development in the industrial workhorse *Trichoderma reesei*. *Proceedings of the National Academy of Sciences* 106(33): 13909-13914

Shin Y. S., Drolet B., Mayer R., Dolence K., Basile F. (2007) Desorption electrospray ionization-mass spectrometry (DESI-MS) of Proteins. *Analytical Chemistry* 79(9): 3514-3518

Simmons E. G. (1977) classification of some cellulase-producing *Trichoderma* species. *Second International Mycological Congress, University of South Florida, Tampa, Florida Abstracts* 2:618, Retrieved from http://www.mycobank.org/MB/324906

Speckbacher V., Zeilinger S. (2018) Secondary metabolites of mycoparasitic fungi. In *Secondary Metabolites – Sources and Applications*. Ramasamy Vijayakumar and Suresh S.S. Raja (eds). IntechOpen, DOI: 10.5772/intechopen.75133.

Taki T., Ishikawa D. (1997) Review: TLC blotting: application to microscale analysis of lipids and as a new approach to lipid-protein interaction. *Analytical Biochemistry* 251: 135-143

Tisch D., Kubicek C. P., Schmoll M. (2011a) New insights into the mechanism of light modulated signalling by heterodimeric G-proteins: ENVOY acts on *gna1* and *gna3* and adjusts cAMP levels in *Trichoderma reesei* (*Hypocrea jecorina*). *Fungal Genetics and Biology* 48: 631-640

Tisch D., Kubicek C. P., Schmoll M. (2011b) The phosducin-like protein PhLP1 impacts regulation of glycoside hydrolases and light response in *Trichoderma reesei*. *BMC Genomics* 12:613

Trail F. (2007) Fungal cannons: explosive spore discharge in the *Ascomycota*. *Federation of European Microbiological Societies (FEMS)* 276: 12-18

Wiseman J. M., Laughlin B. C. (2007) Desorption electrospray ionization (DESI) mass spectrometry: a brief introduction and overview. *Current Separations and Drug Development* 22: 11-14

Yu J. H. (2006) Heterotrimeric G-protein signalling and RGSs in *Aspergillus nidulans*. *The Journal of Microbiology* 44(2): 145-154

Zarzycki P. K., Zarzycka M. B. (2008) Low cost, efficient TLC sprayer. *Journal of Planar Chromatography* 21(3): 221-223

Zeilinger S., Gruber S., Bansal R., Mukherjee P. K. (2016) Secondary metabolism in *Trichoderma* – chemistry meets genomics. *Fungal Biology Reviews* 30: 74-90

7. Supplementary

7.1. G-protein α subunits – GNAs

Supplementary Figure 1. Secondary metabolite production patterns of *T. reesei* G-protein α mutant strains under asexual and sexual conditions. Different visualisation techniques were applied to detect different substances at each panel. **A-C.** Derivatized with anisaldehyde – sulfuric acid, visible light. **D-F.** UV light at 366 nm. Replicates were consistent.

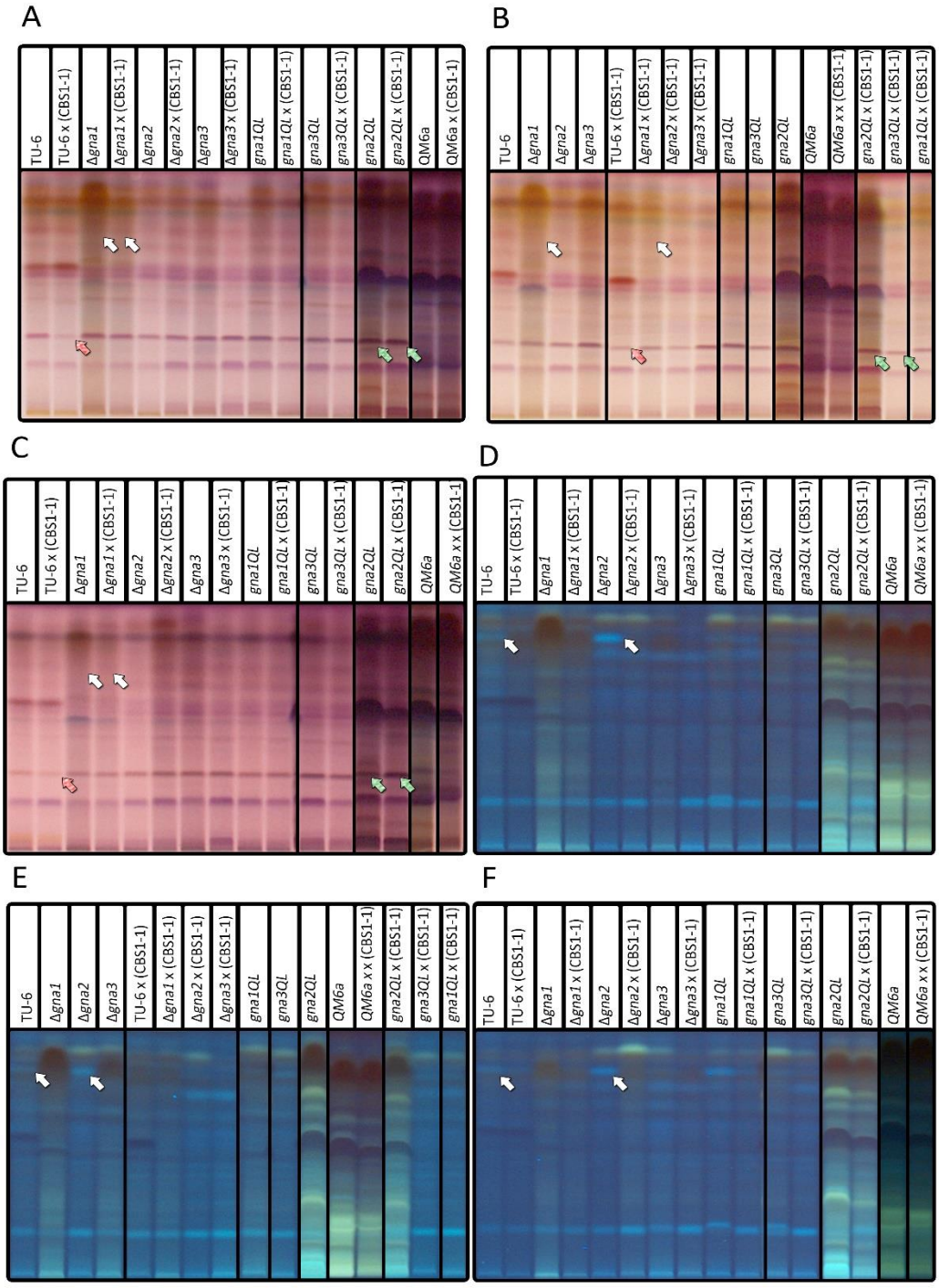

Supplementary Figure 1 (continuation). Secondary metabolite production patterns of *T. reesei* G-protein α mutant strains under asexual and sexual conditions. Different visualisation techniques were applied to detect different substances at each panel. **G-I.** UV light at 254 nm. Replicates were consistent.

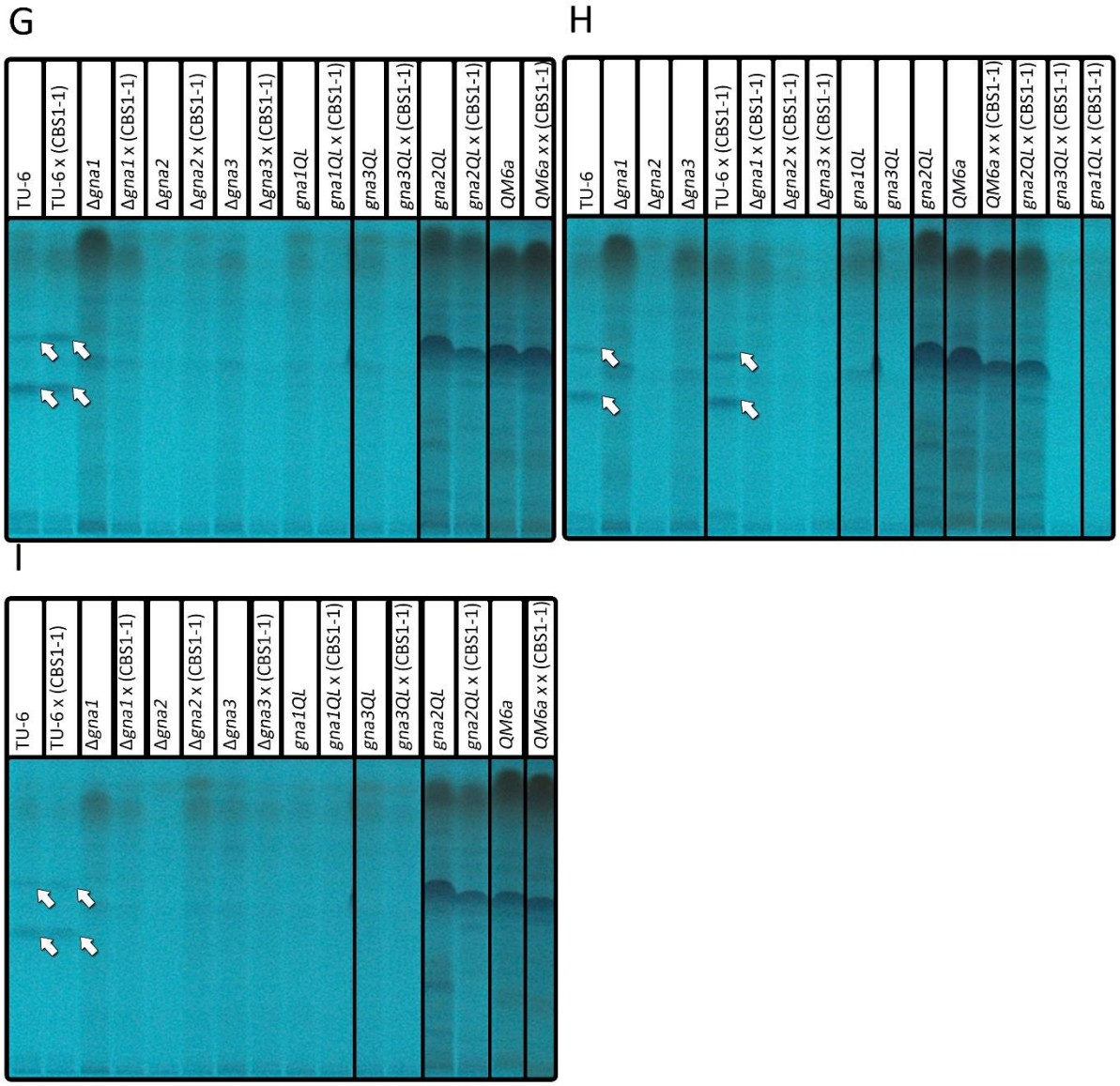

7.2. G-protein ß-γ heterodimer

Supplementary Figure 2. Secondary metabolite production patterns of *T. reesei* G-protein ß, γ subunits and PhLP mutant strains under asexual and sexual conditions. Different visualisation techniques were applied to detect different substances at each panel. **A-C.** Derivatized with anisaldehyde – sulfuric acid, visible light. **D-F.** Derivatized with anisaldehyde – sulfuric acid, UV light at 366 nm. **G-I.** UV light at 366 nm, saturation is altered for better illusion. Replicates were consistent.

.

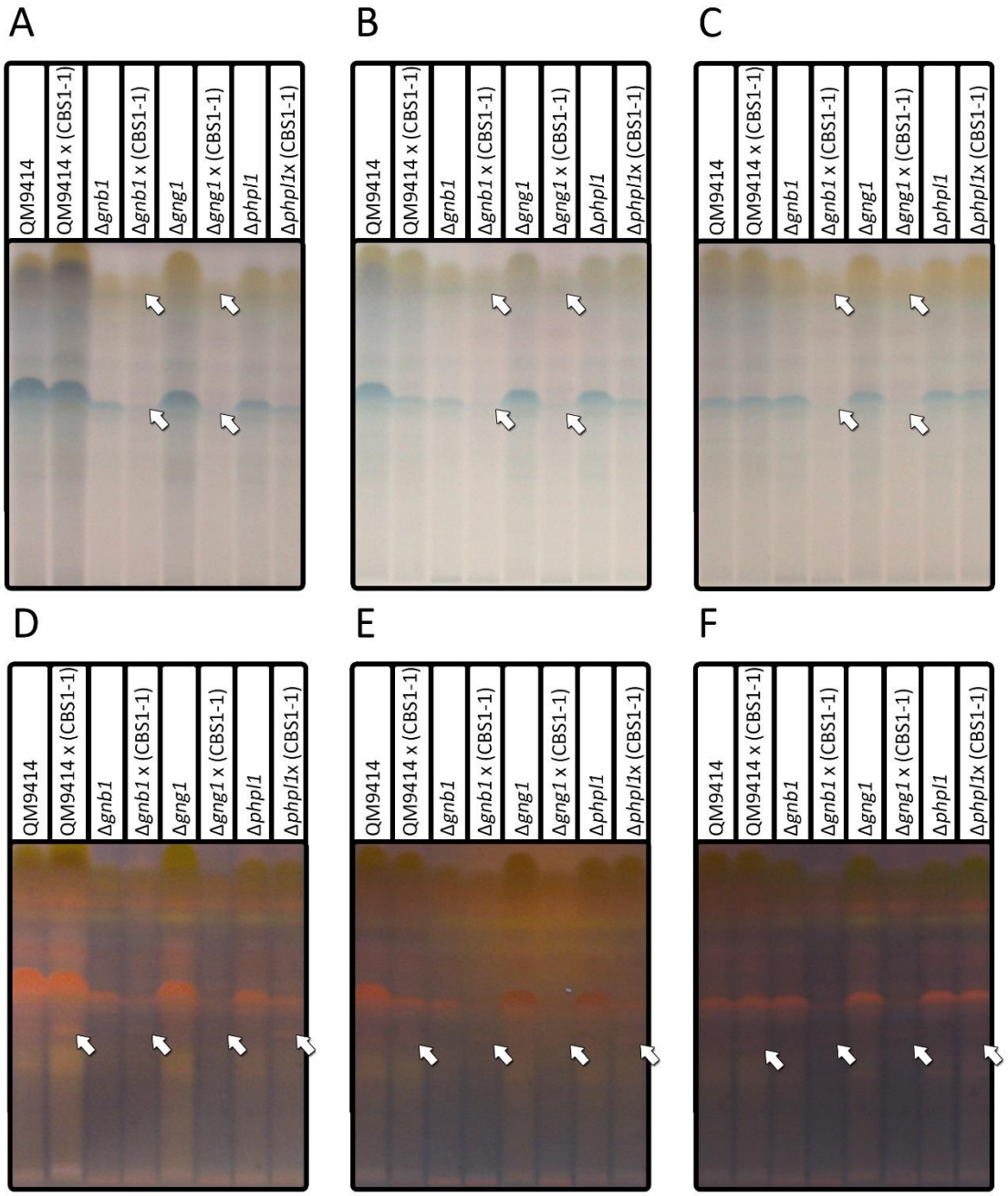

7.3. G-protein coupled receptors and pheromones

Supplementary Figure 3. Secondary metabolite production patterns of *T. reesei* G-protein coupled pheromone receptors and pheromone precursor strains under asexual and sexual conditions. Different visualisation techniques were applied to detect different substances at each panel. **A-C.** Derivatized with anisaldehyde – sulfuric acid, UV light at 254 nm. **D-F.** Derivatized with anisaldehyde – sulfuric acid, visible light. Replicates were consistent.

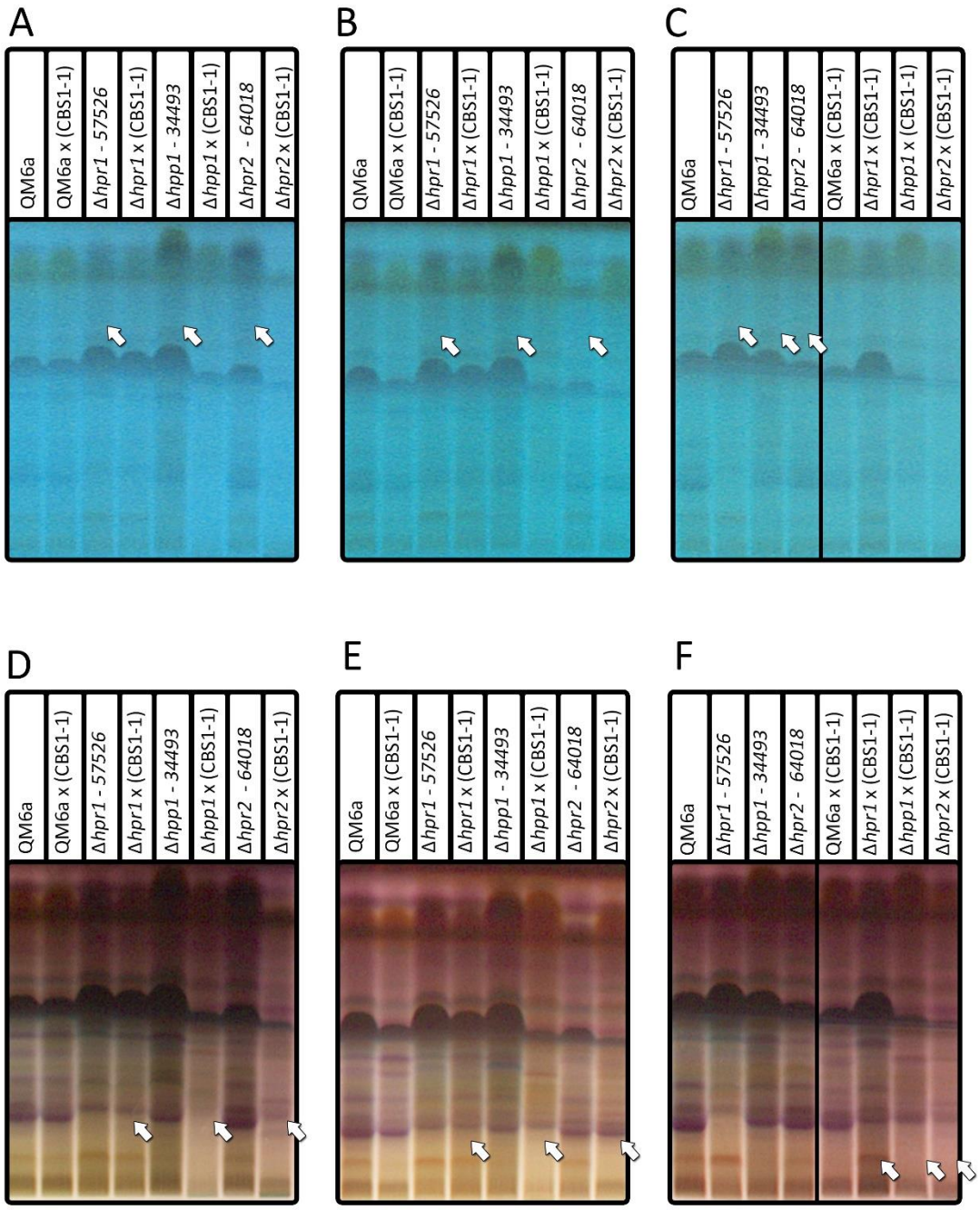

Supplementary Figure 3 (continuation). Secondary metabolite production patterns of *T. reesei* G-protein coupled pheromone receptors and pheromone precursor strains under asexual and sexual conditions. Different visualisation techniques were applied to detect different substances at each panel. **G-I.** Derivatized with anisaldehyde – sulfuric acid, UV light at 366 nm. **J-L.** UV light at 366 nm. Replicates were consistent.